https://doi.org/10.5194/egusphere-2026-573
Preprint. Discussion started: 27 February 2026

Toward robust fine-scale decadal precipitation forecasts through dynamically consistent subsampling

Joanne Couallier[1,2], Didier Swingedouw[2], Charlotte Sakarovitch[1], Ramdane Alkama[2]

[1]LyRE, SUEZ, Pessac, 33600, France
[2]EPOC, Pessac, 33600, France

Correspondence to: Joanne Couallier (joanne.couallier@suez.com)

Abstract. Reliable decadal predictions of regional precipitation are critical for managing water-resources and developing climate services, yet they remain a major challenge. To address this gap, we present a 5-step framework that integrates recent advances in decadal predictions of large-scale sea-level pressure (SLP) modes to enhance prediction skill of precipitation at a fine scale resolution. We first identify key atmospheric indices controlling precipitation variability over France, including the winter and summer North Atlantic Oscillation (NAO), the winter West Atlantic Pressure Anomaly, and the summer Mediterranean-Scandinavia index. These indices are predicted through an improved post-processing method applied on the multi-model Decadal Climate Prediction ensemble. The resulting decadal forecasts of the indices are used to select dynamically consistent members from a large uninitialized climate model ensemble, thereby avoiding initial drift from decadal climate predictions. The selected forecasts are then statistically bias-corrected and downscaled to an 8-km grid, providing relevant predictions for local scale and impact studies. The last step of the framework is the skill evaluation: over France, winter precipitation forecast based on the NAO achieve significant Anomaly Correlation Coefficient across 70% of grid cells. Summer skill, though weaker, improves notably when combining NAO with the Atlantic Multidecadal Variability (significant over 53% of grid cells). This approach offers a transferable pathway toward actionable, fine scale hydroclimate information at the decadal scale, potentially useful for climate services. The methodology is adaptable to other regions and variables, offering promising opportunities for improving decadal-scale hydroclimate predictions.

1 Introduction

Projection of future precipitation remains one of the most challenging aspects of climate science, as they are highly sensitive to the model used (IPCC 2021), the emission scenario considered, and the representation of the internal variability. This internal variability, linked to the intrinsic dynamics of the climate system, introduces substantial uncertainty, particularly at regional scales and on multiyear to decadal timescales (Hawkins and Sutton, 2011). Such uncertainty complicates decision making for water management and climate adaptation, most notably at the decadal scale, a time frame particularly relevant for policymakers. This is especially true over France where precipitation strongly influence hydrological regimes, water management, agriculture, and energy production (IPCC, 2023).

https://doi.org/10.5194/egusphere-2026-573
Preprint. Discussion started: 27 February 2026

Large-scale modes of atmospheric variability exert a strong and spatially structured influence on European precipitation. For example, the North Atlantic Oscillation (NAO) is associated with fluctuations in the jet stream and storm tracks, strongly impacting European climate by producing large anomalies in precipitation and temperature (e.g. Hurrell and Deser, 2010). Its influence on precipitation has been demonstrated in specific French regions, such as the Seine basin during winter months (Friter et al., 2012). Other SLP patterns—including the East Atlantic/Western Russia (EAWRUS), East Atlantic (EA), Scandinavian (SCAND) indices and the West Europe Pressure Anomaly (WEPA)—also modulate seasonal precipitation and extremes across Europe (Casanueva et al., 2014). Variations in WEPA index (Castelle et al. 2017) is exerting particularly strong influence over France (Jalón-Rojas and Castelle, 2021). Additionally, multi-decadal variability in the Atlantic sea surface temperatures—known as the Atlantic Multidecadal Variability (AMV)—affects summer precipitation patterns in Europe via atmosphere-ocean interactions (Börgel et al., 2022; Casanueva et al., 2014; Knight et al., 2006; Simpson et al., 2019; Sutton and Hodson, 2005). These teleconnections link large-scale pressure anomalies to regional hydroclimate variability. Thus, our ability to predict these large-scale modes offers a promising pathway toward more skillful regional precipitation forecasts on decadal timescales (Smith et al., 2020; Borchert et al., 2021).

Decadal climate predictions (DCP) are designed to fill the gap between seasonal forecasts and long-term climate projections (Meehl et al., 2009; Solaraju-Murali et al., 2022). Seasonal forecasts provide initialized climate information up to about 12 months ahead, with skill mainly arising from the initial climate state. Long-term climate projections, in contrast, simulate future climate under external forcing scenarios and do not attempt to predict internal variability at specific dates. DCPs focuses on intermediate timescale: by initializing climate models from the observed state and running them forward for ten years, they combine predictability from both initialization and external forcing, capturing part of the internal climate variability that long-term projections miss (e.g. Swingedouw et al., 2013), but also the role of external forcing from increasing greenhouse gas concentration. Decadal predictions were included in phases 5 and 6 of the Coupled Model Intercomparison Project (CMIP5 and CMIP6) (Boer et al., 2016), as retrospective predictions—called hindcasts—and new forecasts are produced and assessed regularly (Hermanson et al., 2022; World Meteorological Organization., 2024). Decadal hindcasts demonstrate skill for selected variables in certain regions, enabling applications in climate services (Dunstone et al., 2022). Indeed, they can provide actionable information concerning—e.g. North Atlantic hurricane activity for the insurance sector (Lockwood et al., 2023); global wheat yields (Solaraju-Murali et al., 2021); hydropower production (Tsartsali et al., 2023); and drought indices in Germany (Paxian et al., 2022).

Decadal precipitation hindcasts, have demonstrated limited skill over Europe and particularly over France (Hermanson et al., 2022). To address this challenge, recent research (Smith et al., 2020) has focused on improving the prediction of large-scale atmospheric modes that strongly modulate precipitation variability at the continental scale, most notably the NAO. Building on the well-established relationship between the NAO and European precipitation, Smith et al. (2020) proposed an innovative approach: rather than directly predicting regional rainfall, the first step is to skillfully predict the NAO itself. This enables the identification or subsampling of model ensemble members whose atmospheric states are dynamically consistent with the predicted NAO phase, thereby enhancing downstream precipitation forecasts. Building on these advances, a more recent study

https://doi.org/10.5194/egusphere-2026-573
Preprint. Discussion started: 27 February 2026

(Alkama et al., sub.) achieved a further step forward in NAO predictability. This new method is providing enhanced skill of the NAO (Alkama et al., sub.; Smith et al., 2020) and opens new opportunities to apply comparable methods to other large-scale SLP indices shaping Europe's hydroclimate (Hutchins et al., 2025).

Building upon the improved NAO prediction skill, novel approaches have emerged that leverage skillful SLP decadal prediction to enhance precipitation and temperature predictions via methods such as regression models or NAO-matching techniques (Hutchins et al., 2025; Nicolì et al., 2025; Tsartsali et al., 2023). However, these studies primarily focus on winter months and often show limited skill for precipitation over France. Since observed correlations between NAO and precipitation vary spatially and tend to be weaker over parts of France, incorporating additional relevant SLP indices informed by observed precipitation-SLP relationships may improve forecast skill.

This study aims to overcome these limitations by developing a subsampling-based approach that leverages recent advances in NAO prediction skill while integrating additional climate indices chosen to specifically enhance decadal precipitation forecasts over France. Understanding how these large-scale atmospheric modes shape observed precipitation variability is essential for constructing physically consistent and predictable frameworks. In this respect, this framework can also be applied to other regions where one wants to improve decadal prediction skills. Furthermore, by explicitly predicting these indices within initialized decadal forecasts, our approach bridges the gap between large-scale predictability and regional hydrological relevance.

Beyond its scientific value, this work responds to the growing demand from decision-makers and water resource managers for actionable climate information at fine spatial and temporal scales (Sauquet et al., 2025; Gogien et al., 2023). We therefore focus on providing decadal precipitation predictions at approximately 8-km spatial resolution, targeting both winter and summer seasons across regional domains in France. This high-resolution perspective allows us to assess spatial precipitation variability and its linkage to dominant SLP patterns, offering a pathway toward more robust and usable climate information for adaptation planning.

This study is organized as follows: Section 2 describes the data and methods employed; Section 3 presents the evaluation of prediction skill for winter and summer precipitation; Section 4 discusses the results and concludes the study.

2 Data and methods

2.1 Data

2.1.1 Observational Data

The precipitation observational data used in this study are extracted from the SAFRAN (Système d'Analyse Fournissant des Renseignements Atmosphériques à la Neige) analysis, based on the system developed by Météo-France (Durand et al., 1993; Le Moigne et al., 2020). SAFRAN is an operational meteorological analysis scheme that combines ground-based observations, large-scale atmospheric analyses, and orographic information to produce spatially and temporally consistent estimates of near-

https://doi.org/10.5194/egusphere-2026-573
Preprint. Discussion started: 27 February 2026

surface meteorological variables. The dataset provides high-quality precipitation fields at hourly resolution over France, available from 1958 to the present, and is widely used for hydrological and climate studies due to its consistency in time, through homogenization technique, and fine scale detail (~8 km x 8 km resolution).

As described earlier, our predictive framework relies on large-scale atmospheric and oceanic indices, specifically the SLP-based modes and Atlantic Multidecadal Variability (AMV) derived from Sea Surface Temperature (SST) anomalies. For this purpose, we used ERA5 reanalysis dataset (Hersbach et al., 2020), which provides global, high-resolution atmospheric and oceanic fields at 0.25° spatial resolution and hourly temporal frequency. The ERA5 data, covering the period 1948 to the present, offer a physically consistent representation of large-scale climate variability and serve as the observational reference for computing both SLP and SST indices used in this study. The exact definition of those indices will be provided later on in the paper.

2.1.2 Modeled Data

To predict SLP-based mode and AMV indices, we use the multi-model ensemble of initialized decadal predictions from the Decadal Climate Prediction Project Phase A (DCPP-A) within CMIP6 (Boer et al., 2016). The ensemble includes decadal hindcasts from 12 models (see Table A1), with a total of 188 members initialized annually from 1961 to 2014 and run for a decade.

Once the target indices are predicted, we apply a subsampling method (described below) to the outputs from the large ensemble of IPSL-CM6A-LR model, consisting of 32 members covering the period 1850–2059 (Bonnet et al., 2021). IPSL-CM6A-LR model contributed to CMIP6 database. It has a nominal horizontal resolution of approximately 2.5° × 1.25° for the atmosphere and 1° for the ocean. A full description of its main components and climatology can be found in Boucher et al. (2020).

2.2 Methods

The method we propose to obtain fine-scale decadal precipitation forecasting can be summarized in a 5-step workflow (Fig. 1). This method can be applied to any variable to be predicted over any region of the world. It is designed to boost the skill capacity for the prediction of this variable. Here, we describe its application over France for precipitation variable.

The workflow begins with the *selection of a relevant climate index* identified through observed teleconnections between precipitation and atmospheric or oceanic variability. The index is then *predicted* using an approach that is improving raw decadal predictions (Alkama et al., sub.), followed by a *subsampling* procedure that selects the ensemble members from a non-initialized climate model that are best matching the index forecasted. The resulting subset of simulations then undergoes temporal aggregation and statistical downscaling to generate regional-scale precipitation forecasts. Finally, these forecasts are evaluated against observations using deterministic and probabilistic skill scores. This workflow is applied in this paper to build and evaluate improved precipitation predictions separately for extended-winter (October to March) and extended-summer (April to September). The five key steps are detailed below:

https://doi.org/10.5194/egusphere-2026-573
Preprint. Discussion started: 27 February 2026

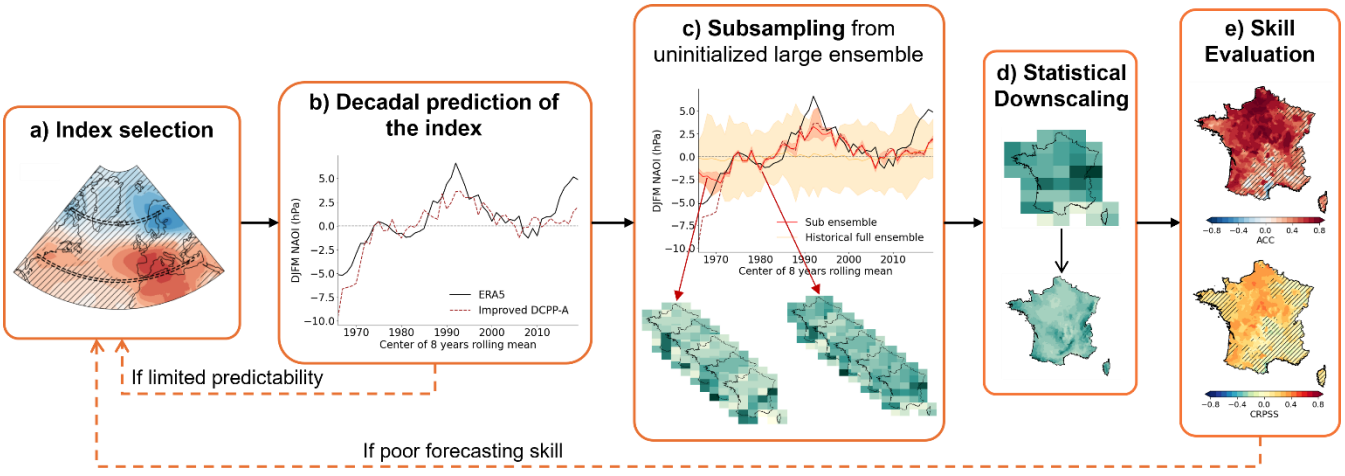

Figure 1: Schematic workflow of the proposed framework for decadal prediction of hydroclimate variables: (a) identifying the most relevant large-scale index (here, wNAO), showing the strongest correlation with the target hydroclimate variable (here, winter precipitation); (b) predicting the selected index using improved decadal forecasts from the DCPP database; (c) selecting ensemble members from a uninitialized climate model that best reproduce the predicted index; (d) aggregating, bias-correcting and downscaling the resulting sub-ensemble predictions to the 8-km spatial resolution; (e) Evaluating forecasts skill using temporal metrics (e.g. ACC and CRPSS).

a. Index selection

To identify large-scale drivers of precipitation variability over France, we derive the main SLP pattern that affect precipitation. Then, we combine the results with knowledge from literature-based climate indices. More precisely, the whole process is following the three analytical stages described below.

a.1 Identifying dominant precipitation patterns

We apply Empirical Orthogonal Function (EOF) analysis to observed seasonal precipitation anomalies using the eofs Python package (Dawson, 2016). EOF analysis decomposes the covariance matrix of the input data into orthogonal spatial patterns (EOFs) and their corresponding time series called principal components (PCs) (Wilks, 2011).

To emphasize low-frequency variability and reduce the influence of interannual noise, precipitation anomalies are smoothed using a 3-year centered rolling mean, and linear trends are removed. The choice of the averaging window is a compromise between enhanced low-frequency variability and retaining sufficient temporal resolution. Results were qualitatively similar for averaging windows between 2 and 4 years (not shown). We define two 6-month extended seasons: October to March (ONDJFM) and April to September (AMJJAS). We limit our analysis to the first two leading modes of variability from the EOF analysis.

a.2 Exploring main temporal periodicities

https://doi.org/10.5194/egusphere-2026-573
Preprint. Discussion started: 27 February 2026

To gain physical understanding of the main mode of variability obtained through EOF, it is interesting to evaluate the frequency of the main variability modes of precipitation over France. Indeed, strong low frequency variability is indicative of some potential for decadal predictability. Although this step is not required in our workflow, it was included in this study to better characterize the variability of precipitation over France, and to explore how this might relate to decadal predictability. The frequencies characteristics are further investigated by applying a continuous wavelet transform (CWT) to the first two principal components using the pycwt Python package (Krieger and Freij, 2023; Torrence and Compo, 1998) with a Morlet wavelet. Wavelet analysis allows the examination of multiscale and non-stationary signals by convolving the input time series with scaled and shifted versions of the wavelet. Time-averaged frequency spectra highlight dominant frequencies, while the full CWT spectra show their temporal evolution.

a.3 Linking precipitation to large-scale climate patterns

We compute correlation maps between the first two principal components of precipitation anomalies (PCs) and SLP anomalies over the North Atlantic sector (20°-85°N, 85°W-40°E), for both extended warm and cold seasons. The significance of the correlation coefficients is assessed using a block bootstrap procedure (1000 samples) with a block size of 3 years, where correlations are considered significant if zero is outside the 95% confidence interval of the bootstrap distribution. Based on the significant correlation patterns and previous literature, candidate SLP indices for decadal precipitation prediction are identified (see Section 3.1 for further discussion). From these patterns and previous literature, we identified four atmospheric indices most relevant for France:

For the winter season, those are:

- The North Atlantic Oscillation Index (wNAO), calculated for DJFM (December to March) as the difference in mean SLP between two zonal boxes spanning the North-Altantic-European sector—subtropical (35°-40°N, 80°W-30°E) and subpolar (63°-67°N, 80°W-30°E)—following Jianping and Wang (2003). This formulation reduces sensitivity to east-west shifts in the centers of action that can happen within climate models.
- The West Europe Pressure Anomaly (wWEPA), defined for ONDJFM (October to March) as the SLP difference between two large spatial boxes: one centered on the Canary Islands (22°-36°N, 27°-0°W) and another over England (47°-61°N, 21°W-21°E). This index based on regional boxes is inspired by the WEPA station-based index of Castelle et al. (2017) but is less sensitive to slight shifts in space, making it more robust for observations and models.

For the summer season, they are:

- The Summer North Atlantic Oscillation index (hereafter sNAO), defined for AMJJAS (April to September) as the sea level pressure (SLP) difference between two regions: one located west of England and France (45°–55°N, 20°W–12°E) and another south of Greenland (55°–69°N, 60°–45°W). This definition is adapted from previous studies (Wang and Ting, 2022; Dunstone et al., 2023; Folland et al., 2009) to better capture the observed correlations between precipitation principal components and SLP.

https://doi.org/10.5194/egusphere-2026-573
Preprint. Discussion started: 27 February 2026

- The Mediterranean-Scandinavia index (sMedScand), computed for AMJJAS (April to September) as the difference between a region over the Mediterranean (30°-46°N, 6°W-35°E) and a region over Scandinavia (55°-70°N, 3°-22°E), based on the obtained correlations between the second PC of summer precipitation and SLP.

The relevance of these indices is evaluated by computing Pearson correlation coefficients with the corresponding principal components at two temporal scales. Correlations are first computed between the PCs based on 3-year mean precipitation and the climate indices smoothed using a 3-year rolling mean. Then, lower-frequency variability of around 8 years is assessed by applying another 6-year rolling mean to the previous PCs and 3-year means climate indices.

In addition to the atmospheric indices, we include an AMV index to capture potential low-frequency oceanic influences on European climate (Sutton and Hodson, 2005). The AMV describes the evolution of the dominant mode of North Atlantic SST variability over multidecadal timescales (Schlesinger and Ramankutty, 1994). We define the index used here as the spatial mean of North Atlantic SST over 0°–60°N, 76°W–0°E. To avoid making any hypothesis to remove the global warming trend, we just use this raw and unadjusted times series that we call uAMV (e.g. Michel et al., 2022) since this does not correspond to classical definitions from the literature, where the trend is removed using various different approaches (e.g. Trenberth and Shea, 2006, Terray, 2012) . We retain here the externally forced signal in the uAMV index as well as the internal signal, because both signals are used in the subsampling procedure described below (section 2.2.c) to select model members that best reproduce both internal variability and forced trends, which may be misrepresented in models (Kharin et al., 2012). Removing the forced component consistently across observations, initialized, and uninitialized simulations is challenging; thus, keeping the raw signal improves consistency and preserves important multidecadal trends.

b. Predicting climate indices using boosted decadal forecasts

We apply the post-processing method developed by Alkama et al. (sub.) that improve the earlier work by Smith et al. (2020) and Marcheggiani et al. (2023). This approach includes two key steps:

1. Aggregating decadal predictions optimally by combining members from previous start dates to increase the ensemble size.
2. Rescaling the forecast to match the observed variance of the predicted signal.

The resulting predictions are named “boosted” decadal predictions to distinguish them from the raw DCP ensemble. Here, the method is applied for lead times from 2 to 9 years to predict 8-year mean indices. For some indices (wWEPA, sNAO, and wMedScand), the predicted trends are opposite in sign to those observed (Fig. S1.1). To correct this bias, the linear trend in the prediction is adjusted to match the observed trend (following approach from e.g. Kharin et al., 2013). For future forecasts, this correction can be applied by extending this historical observed trend into the next decade. This post-processing method allows to improve the decadal prediction forecast skill.

https://doi.org/10.5194/egusphere-2026-573
Preprint. Discussion started: 27 February 2026

c. Subsampling procedure (index-matching)

To transfer predictability from large-scale indices to precipitation, we adopt an index-based subsampling strategy inspired by the NAO-matching method (Smith et al., 2020; Alkama et al., submitted). Smith et al. (2020) introduced the NAO-matching method by selecting a subset of 20 members from multi-model decadal simulations at each 8-year window whose NAO values best match the NAO prediction from the whole DCP predictions ensemble mean. Climate variables (e.g., precipitation) are then extracted from this subset, yielding "NAO-matched precipitation" predictions expected to improve skill.

Alkama et al. (sub) applied NAO-matching to an uninitialized large ensemble from CEMS2, showing skill improvements compared to initialized multi-model, also subsampled on NAO predictions, especially in extended-winter precipitation, though with limited skill over France. This might be related to the fact that initialized predictions can show strong drift in the first few years, contrary to uninitialized large ensemble (e.g. Polkova et al., 2023).

Motivated by these findings, we apply the subsampling method to the large ensemble of extended historical IPSL-CM6A-LR model (32 members), spanning 1850-2059 (Bonnet et al., 2021), hereafter called "uninit IPSL". The subsampling method selects relevant uninitialized ensemble members separately for each 8-year mean window. The 8-year mean climate index centered in t is predicted by each 32 uninitialized ensemble members ($u_i(t), \forall\, i \in [1, 32]$), and by the boosted DCP ensemble mean ($f(t)$). We select the five uninitialized ensemble members minimizing D defined as:

$$D_i(t) = \sqrt{\left(u_i(t) - f(t)\right)^2}, \forall\, i \in [1, 32] \quad (1)$$

We name "Sub(X)" the selected ensemble where X denotes the climate index used (e.g., Sub(wNAO)). The procedure can be applied using any SLP or SST index individually or combined. In the case of combined selection, the five selected uninitialized ensemble members minimize:

$$D_i(t) = \sqrt{\alpha \times \left(u1_i(t) - f1(t)\right)^2 + \beta \times \left(u2_i(t) - f2(t)\right)^2}, \forall\, i \in [1, 32],\ \alpha = \beta = 1 \quad (2)$$

For extended summer precipitation prediction, we combine the sNAO, sMedScand SLP indices and the uAMV. The corresponding selected ensembles are called "Sub(sNAO+uAMV)" and "Sub(sMedScand+uAMV)". The subsampling procedure is applied on the entire historical period from 1961 to 2024, allowing to extract precipitation—or other variables—predictions from the selected ensembles. The skill of this system is assessed on 8-year means computed from ensemble members that can be different at successive 8-year periods. The resulting prediction shows reduced temporal coherence that is not directly comparable to the smoothed rolling means applied to observations. To ensure consistent autocorrelation properties, we apply the post-processing method described above (part 2.2.b) to the selected members.

https://doi.org/10.5194/egusphere-2026-573
Preprint. Discussion started: 27 February 2026

d. Statistical downscaling

The SAFRAN reanalysis provides high-quality precipitation observations at an 8 km resolution across France and has become a reference dataset for hydrological applications, water resource management, and impact studies (Labrousse et al., 2020; Seyedhashemi et al., 2023; Vidal et al., 2010). Developing decadal precipitation forecasts at the same spatial scale would directly support these operational needs by bridging the gap between coarse-scale climate predictions and local-scale decision-making. Correcting the bias of the prediction is also necessary in order to use them in impact studies.

To achieve this, we use the Cumulative Distribution Function-transform (CDF-t) method (Michelangeli et al., 2009), a widely used quantile-mapping technique. CDF-t adjusts the statistical distribution of modeled precipitation to match that of observations while preserving the model's representation of large-scale variability.

This method is allowing to statistically downscale the subsampled precipitation outputs (~150 km resolution) onto the SAFRAN 8-km grid using available observation. Such an approach is necessary and widely used for impact studies.

This method also accounts for changes in the distribution between historical and forecast periods through a transfer function that aligns modeled and observed daily cumulative distributions and therefore remove the bias in prediction at the daily timescale. The CDF-t technique has been extensively validated for precipitation bias correction and regional climate projection studies (Gogien et al., 2023; Sauquet et al., 2025; Vrac et al., 2012).

e. Skill evaluation

We assessed the skill of 8-year precipitation predictions against SAFRAN observations using deterministic and probabilistic metrics (see details in Appendix B). Those skill scores are:

- Anomaly Correlation Coefficient (ACC): It measures the ability of the ensemble mean to predict temporal variations of observed precipitation anomalies (Wilks, 2011).
- Residual Correlation Coefficient (RCC): It quantifies added value of initialization compared to the uninitialized ensemble mean. Correlations are computed between residuals from two regressions allowing to withdraw the uninitialized ensemble mean from observations and predictions (Smith et al., 2019).
- Continuous Ranked Probability Score (CRPS): It assesses overall probabilistic forecast quality by integrating squared differences between the forecasted and observed cumulative distribution functions (Gneiting and Raftery, 2007; Hersbach, 2000). CRPS quantifies both calibration and sharpness as a forecast will be penalized if the observed value falls outside the predicted interval, or if the interval is too wide. The CRPS is computed using the scores Python package (Leeuwenburg et al., 2024), with the 'fair' method to correct for finite-ensemble bias (Ferro, 2014).
- CRPS Skill Score (CRPSS): Compare CRPS of the subsampled predictions against the full uninitialized ensemble. CRPSS and its categorical version RPSS (Ranked Probability Skill Score) are commonly used to evaluate

https://doi.org/10.5194/egusphere-2026-573
Preprint. Discussion started: 27 February 2026

probabilistic climate forecasts (Bonnet et al., 2025; Goddard et al., 2013; Moulds et al., 2023). In our case the continuous version is used.

Statistical significance of ACC, RCC and CRPSS is assessed using a block bootstrap with 1,000 samples and block size of eight years to account for temporal autocorrelation (Rousselet et al., 2021; Smith et al., 2020). Scores are considered significant if the probability of being below zero is less than 0.05 (Goddard et al., 2013).

Before evaluating forecast skill, the variance of both the subsampled predictions and the uninitialized full ensemble are rescaled to match that of the observations. Because observations represent a single realization of the climate system, while ensemble means (five-member subsampled and 32-member uninitialized) inherently smooth variability through averaging, their standard deviations are artificially reduced. To ensure statistical consistency and comparability with the observed variance, we apply a variance-scaling correction. Each ensemble member is multiplied by σ_o/σ_m, where σ_o and σ_m are the standard deviations of the observations and the ensemble member, respectively, computed on the entire historical period. This adjustment does not affect ACC but improves CRPSS by preventing prediction ensemble from being too narrow, which would lead to underconfident forecast. CRPSS maps computed from the raw, uncorrected predictions are provided in the supplementary material (Fig. S6.2).

3 Results

3.1 Observed large-scale variability and teleconnections

The EOF analysis of observed precipitation anomalies (Fig. 2 and 4) reveals distinct spatial and temporal modes of variability over France for both winter and summer seasons. For winter (October to March), the first EOF explains 50.2% of the total variance and exhibits a spatially coherent pattern with uniform sign across most of France, except along the Mediterranean coast (Fig. 2a). This indicates a dominant large-scale mode of variability for precipitation that affects almost the whole France. The second mode accounts for an additional 18% of the variance and displays a pronounced North-South dipole, reflecting opposite sign of variability between northern and southern France (Fig. 2b).

https://doi.org/10.5194/egusphere-2026-573
Preprint. Discussion started: 27 February 2026

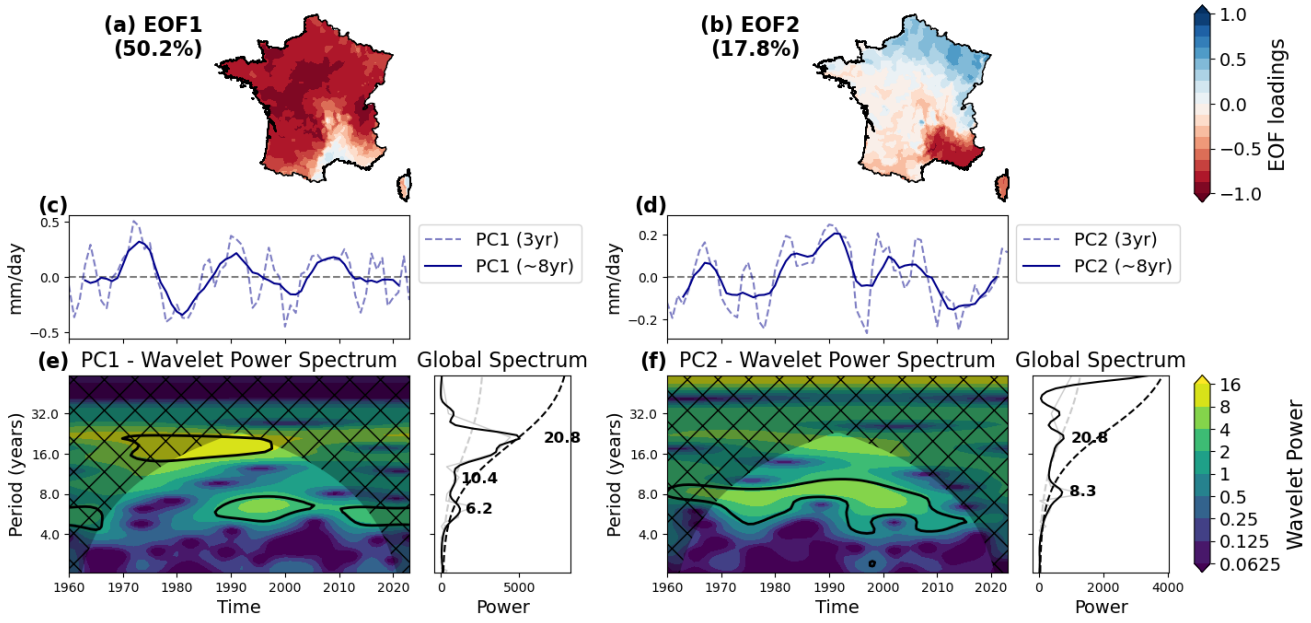

Fig. 2: Spatial and temporal variability of winter (ONDJFM) precipitation over France (1960-2023). Panels (a) and (b) show the spatial patterns of the first two Empirical Orthogonal Function (EOF) modes of 3-year running mean winter precipitation anomalies from SAFRAN observations, with the percentage of total variance explained shown in parentheses. Colors represent the spatial loadings of each mode expressed as correlations with the principal components. Panels (c) and (d) depict the corresponding principal components (PCs) time series in mm/day, with dashed and solid blue lines denoting the raw PCs from 3-year means and the low-frequency filtered PCs of around 8 years, respectively. Panels (e) and (f) present the wavelet power spectra (left) and global wavelet power spectra (right) for EOF1 and EOF2 PCs, respectively. In the wavelet spectra, the x-axis is time, and the y-axis is period in years; warmer colors denote higher power. Black contours in the wavelet spectra indicate the 95% confidence level against a red noise background, while shaded regions depict the cone of influence (COI) where edge effects may influence the results. The global spectra panels show the time-averaged wavelet power spectrum (solid black line) and the Fourier power spectrum (solid gray line), with dashed lines corresponding to the 95% significance levels.

Wavelet analysis of the first Principal Component (PC1) identifies two statistically significant periodicities close to 6 and 21 years (Fig. 2e). The longer ~21-year cycle remains persistent throughout the historical period, whereas the ~6-year periodicity varies in strength over time. The second PC (PC2) shows a more stable oscillation with a period close to 8 years (Fig. 2f). Together, these statistically significant multi-annual to multi-decadal oscillations reveal physically consistent, non-stationary modes of variability. It suggests that a portion of winter precipitation might be linked to slowly evolving oceanic variability mode—since the ocean has far more temporal inertia than the atmosphere—such as over the North Atlantic region (Persechino et al., 2013). Since the timeseries provided by SAFRAN covers less than 70 years, peaks of variability beyond 30 years are not captured by this analysis. A bi-decadal variability mode in the North Atlantic has been highlighted in the northern part of the North Atlantic Ocean (Swingedouw et al., 2013, 2015) and might explain the 21-year peak highlighted here, through imprints of the ocean on the atmosphere.

Correlation maps between winter precipitation PCs and North Atlantic SLP anomalies reveal robust teleconnection patterns in the atmosphere (Fig. 3). Correlation map of SLP with PC1 of precipitation displays a dipole pattern over the North Atlantic-European sector that closely mirrors the WEPA index defined by Castelle et al. (2017). A positive WEPA corresponds to an

https://doi.org/10.5194/egusphere-2026-573
Preprint. Discussion started: 27 February 2026

intensification and southward shift of the Icelandic Low-Azores High dipole, which drives enhanced precipitation across western and central Europe (Jalón-Rojas and Castelle, 2021). Correlation map of SLP with PC2 of precipitation shows a broader pattern consistent with the wNAO pattern. Time series comparisons confirm strong negative correlations between PC1 and wWEPA (r=-0.75, p<0.01 for 3-year smoothing), and more moderate positive correlations between PC2 and wNAO (r=0.43, p<0.01). These relationships justify using wWEPA and wNAO as key predictors for winter precipitation variability.

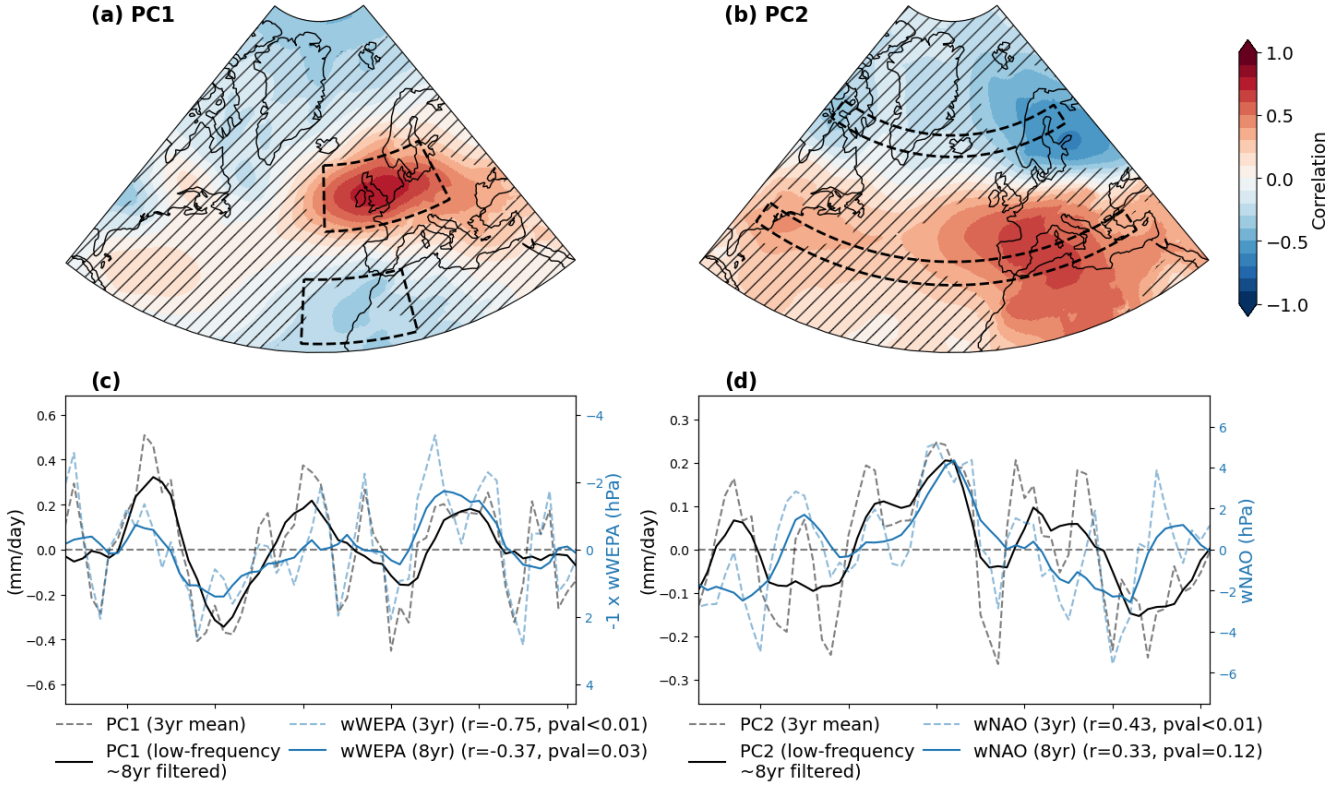

Fig. 3: Relationship between winter (ONDJFM) precipitation variability and large-scale North Atlantic atmospheric circulation. Panels (a) and (b) display spatial correlation between the first two precipitation PCs (PC1 and PC2) and SLP anomalies over the North Atlantic. Hatched areas denote statistically non-significant correlations at the 95% confidence level based on a block-bootstrap test. Black dashed boxes outline the spatial domains used to compute the wWEPA (panel a) and wNAO indices (panel b). Panels (c) and (d) compare the time series of precipitation PCs (black lines) with their corresponding SLP indices (blue lines), including 3-year running mean (dashed) and low-frequency (~8-year) filtered (solid). Reported correlation coefficients (r) correspond to both smoothing scales. Units for the precipitation PCs are mm/day, for the SLP indices are hPa.

For summer (April–September), the first EOF of precipitation over France explains 50% of the variance and show uniform pattern across France, except over the Mediterranean coast (Fig. 4a). The second mode (17%) again exhibits a North-South dipole (Fig. 4b). Wavelet analysis of the PC1 highlights a notable ~7-year periodicity since the mid-1980s, while the PC2 exhibits a strong 21-year oscillation alongside an intermittent 5-year cycle.

https://doi.org/10.5194/egusphere-2026-573
Preprint. Discussion started: 27 February 2026

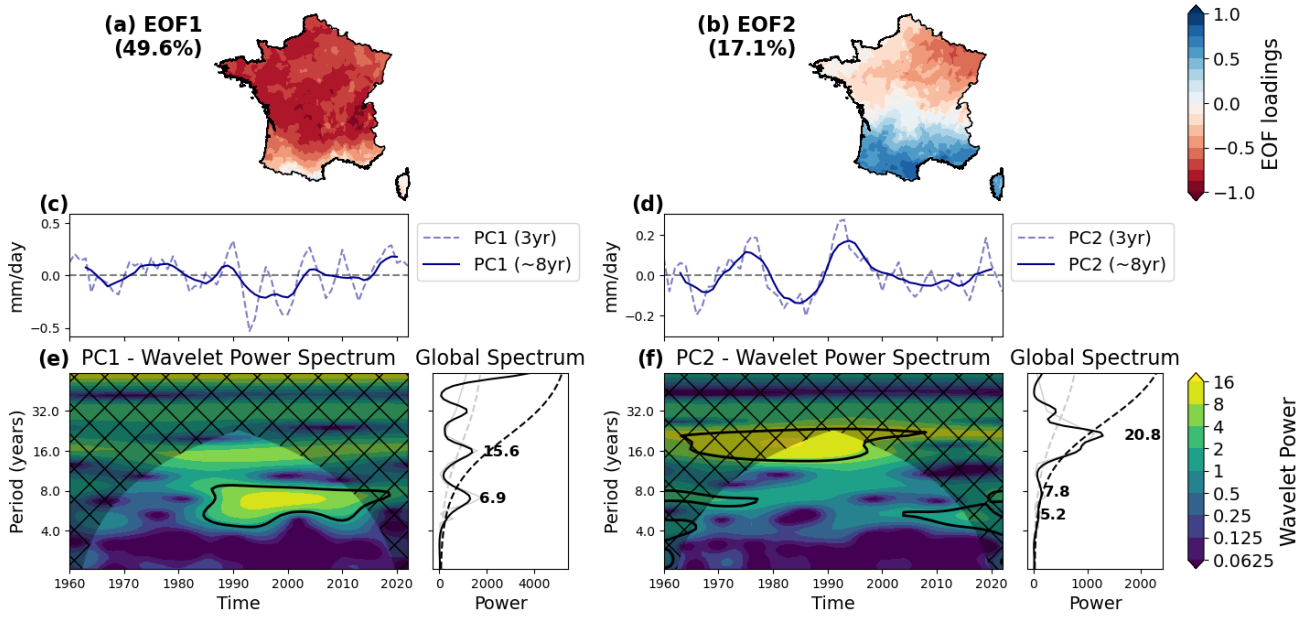

Fig. 4: Spatial and temporal variability of summer (AMJJAS) precipitation over France (1960-2023). Panels (a) and (b) show the spatial patterns of the first two Empirical Orthogonal Function (EOF) modes of 3-year running mean summer precipitation anomalies from SAFRAN observations, with the percentage of total variance explained shown in parentheses. Colors represent the spatial loadings of each mode expressed as correlations with the principal components. Panels (c) and (d) depict the corresponding principal components (PCs) time series in mm/day, with dashed and solid blue lines denoting the raw PCs from 3-year means and the low-frequency filtered PCs of around 8 years, respectively. Panels (e) and (f) present the wavelet power spectra (left) and global wavelet power spectra (right) for EOF1 and EOF2 PCs, respectively. In the wavelet spectra, the x-axis is time, and the y-axis is period in years; warmer colors denote higher power. Black contours in the wavelet spectra indicate the 95% confidence level against a red noise background, while shaded regions depict the cone of influence (COI) where edge effects may influence the results. The global spectra display the time-averaged wavelet power (solid black line) and the Fourier power (solid gray line), with dashed lines corresponding to the 95% significance levels.

Correlations between summer PCs and SLP anomalies show that PC1 is linked to the Summer NAO (sNAO) pattern, whose index definition is here a bit refined compared to standard one, in order to better align with main driver of precipitation variability (Fig. 5a, c). Generally speaking, the sNAO pattern is smaller in scale and shifted northward as compared to the winter NAO. Although the amplitude is weaker, it significantly influences northern European climate through modulation of the North Atlantic jet streams and storm tracks (Dong et al., 2013; Dunstone et al., 20 23; Folland et al., 2009). The resulting sNAO index is strongly correlated with PC1 ($r=0.74$, $p<0.01$ for 3-year smoothing). PC2 exhibits weaker correlations with SLP but highlights two significant regions over the Mediterranean and Scandinavian regions, motivating the definition of a Mediterranean-Scandinavia (sMedScand) index (Fig. 5b, d). The sMedScand index is negatively correlated with PC2 ($r=-0.46$, $p<0.01$ for 3-year smoothing).

https://doi.org/10.5194/egusphere-2026-573
Preprint. Discussion started: 27 February 2026

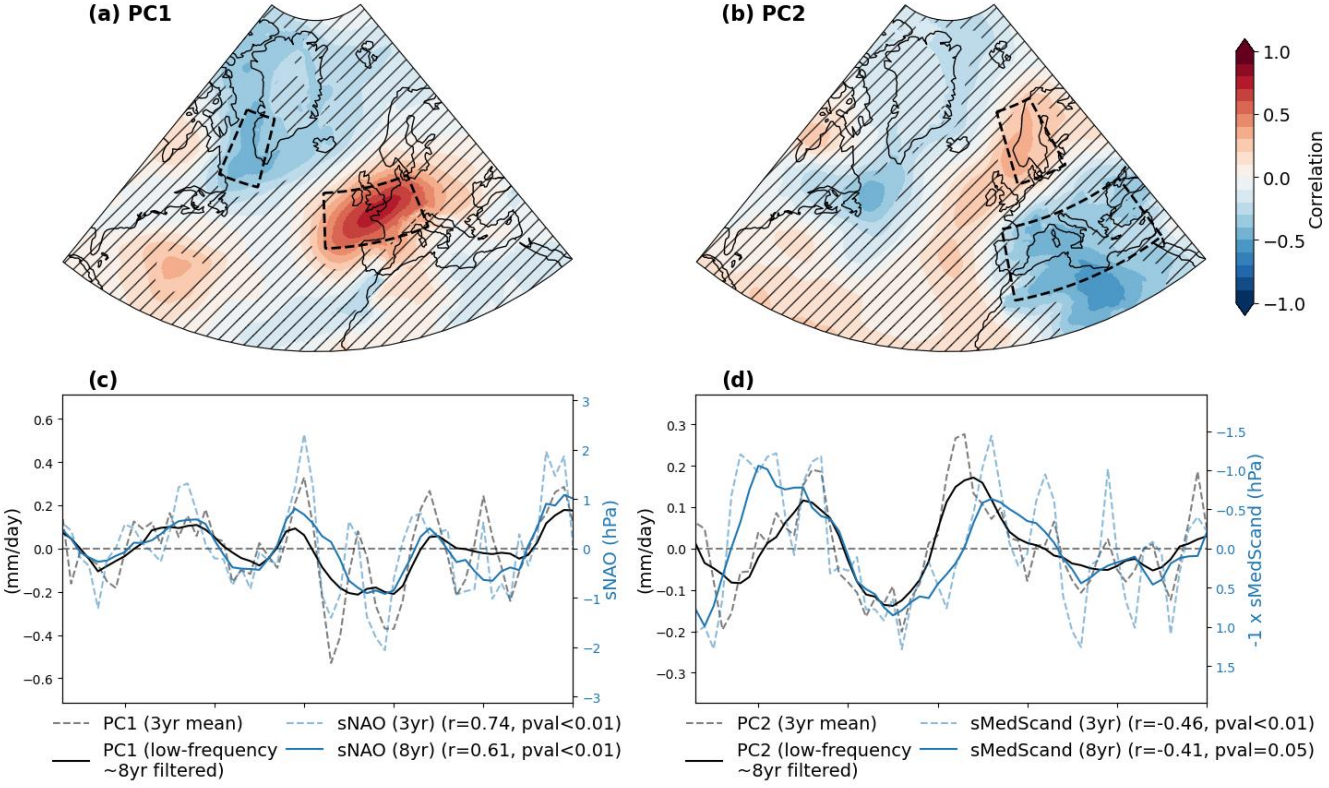

Fig. 5: Relationship between summer (AMJJAS) precipitation variability and large scale North Atlantic circulation. Panels (a) and (b) show the correlation patterns between summer precipitation PCs (PC1 and PC2) and SLP anomalies over the North Atlantic. Hatched areas indicate regions where correlations are statistically significant at the 95% confidence level based on a block-bootstrap test. Black dashed boxes outline the spatial domains used to compute the sNAO (panel a) and sMedScand indices (panel b). Panels (c) and (d) compare the time series of precipitation PCs (black lines) and their corresponding SLP indices (blue lines), including 3-year running mean (dashed) and low-frequency (~8-year) filtered (solid). Reported correlation coefficients (r) correspond to both smoothing scales. Units for the precipitation PCs are mm/day, and for the SLP indices are hPa.

3.2 Decadal prediction skill of atmospheric and oceanic indices

Hindcasts from the boosted Decadal Climate Prediction Project (DCPP) ensemble successfully reproduce the observed low-frequency variability (8 years) of the key atmospheric indices selected above (Fig. 6 and 7).

https://doi.org/10.5194/egusphere-2026-573
Preprint. Discussion started: 27 February 2026

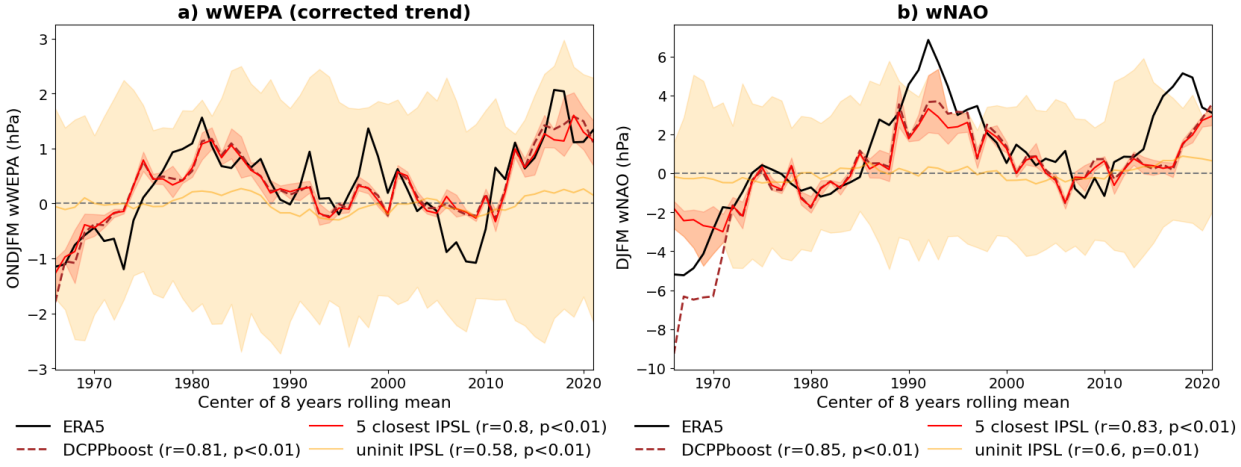

Fig. 6: Observed and predicted decadal variability of winter atmospheric indices. Panels (a) and (b) show 8-year running mean of the wWEPA and wNAO indices for extended winter seasons (ONDJFM and DJFM respectively). The black line represents ERA5 reanalysis, while the burgundy dashed line shows predictions from the boosted DCPP method. The red shading indicates the spread of the five subsampled members, best matching DCPP indices and selected from the uninitialized IPSL-CM6A-LR ensemble in each 8-year time window, with the bold red line marking their ensemble mean. The yellow line and shading represent the mean and full spread (minimum to maximum) of the entire uninitialized IPSL ensemble, respectively. Correlation coefficients and p-values between predictions and observations are reported in parenthesis of each panel's legend.

For winter, boosted DCPP hindcast effectively capture the observed low-frequency variability of both the wWEPA and wNAO indices, with correlation coefficients of 0.81 and 0.85, respectively (Fig. 6). Subsampling the five closest members to the boosted hindcasts in terms of SLP indices from the uninitialized IPSL ensemble results in predictions closely matching the boosted forecasts. The full uninitialized IPSL ensemble shows moderate skill with wider uncertainty and less agreement with observations (Fig. 6). Correcting the trend of the wWEPA index notably improves forecast correlation by mitigating model drift effects. Importantly, wNAO predictability is higher when focusing on the 4-month extended winter (December to March) period, as forecast skill diminishes when extending the season to the 6-month ONDJFM period, underscoring the importance of seasonal selection for skill assessment. We therefore use in the following the prediction of wNAO over this DJFM season.

For summer, the boosted forecasts indicate skill for both sNAO (ACC=0.72) and sMedScand (ACC=0.57) (Fig. 7a, b). The skill is even higher for the uAMV (ACC=0.94; Fig. 7c) index, reflecting the longer persistence of oceanic modes and their high predictability (e.g. (Msadek et al., 2010; Persechino et al., 2013). All boosted decadal predictions ACCs outperform corresponding uninitialized IPSL ensembles substantially.

https://doi.org/10.5194/egusphere-2026-573
Preprint. Discussion started: 27 February 2026

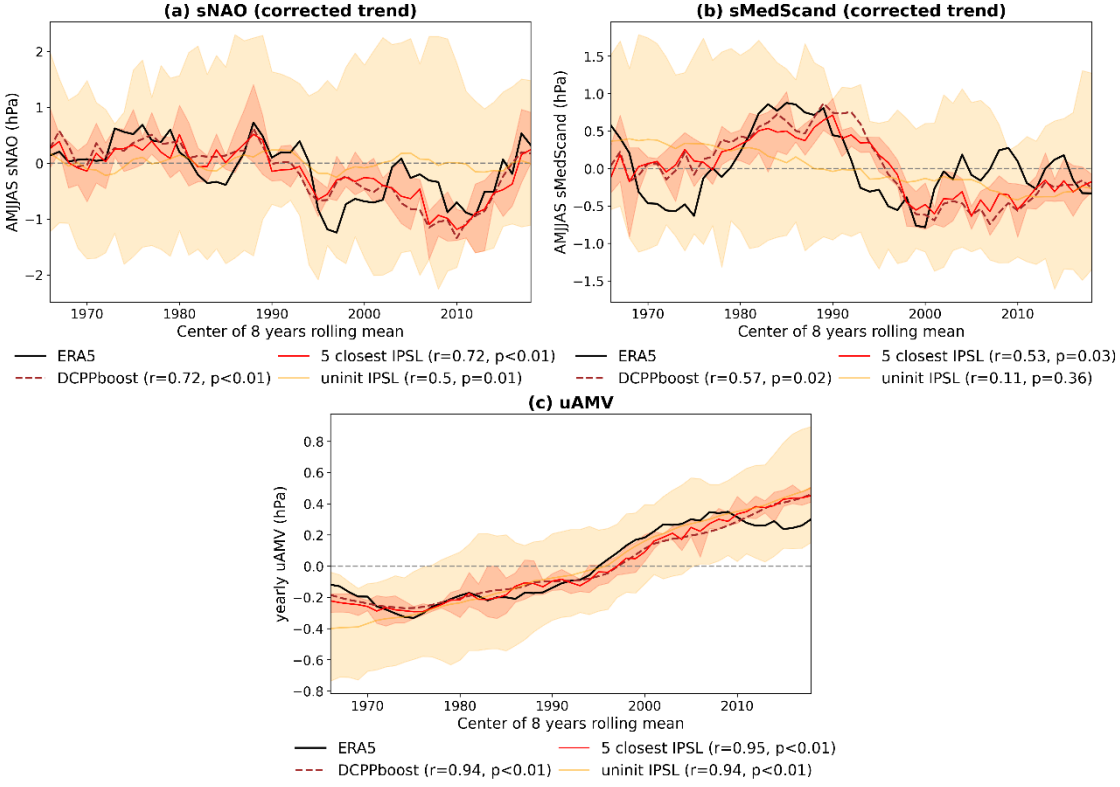

Fig. 7: Observed and predicted decadal variability of summer atmospheric indices. Panels (a) and (b) show 8-year running mean of the sNAO and sMedScand indices for the extended summer season (AMJJAS), and panel (c) shows 8-year running mean of the uAMV. The black line represents ERA5 reanalysis, while the burgundy dashed line shows predictions from the boosted DCPP method. The red shading indicates the spread of the five subsampled members, best matching DCPP indices and selected from the uninitialized IPSL-CM6A-LR ensemble in each 8-year time window, with the bold red line marking their ensemble mean. The yellow line and shading represent the mean and full spread (minimum to maximum) of the entire uninitialized IPSL ensemble, respectively. Correlation coefficients and p-values between predictions and observations are reported in parenthesis of each panel's legend.

3.3 Seasonal precipitation forecast skill

Precipitation hindcasts, derived from the subsampling approach, are analyzed in Fig. 8 and 9 and do show skillful prediction over the past periods in a number of regions of France both in summer and winter.

https://doi.org/10.5194/egusphere-2026-573
Preprint. Discussion started: 27 February 2026

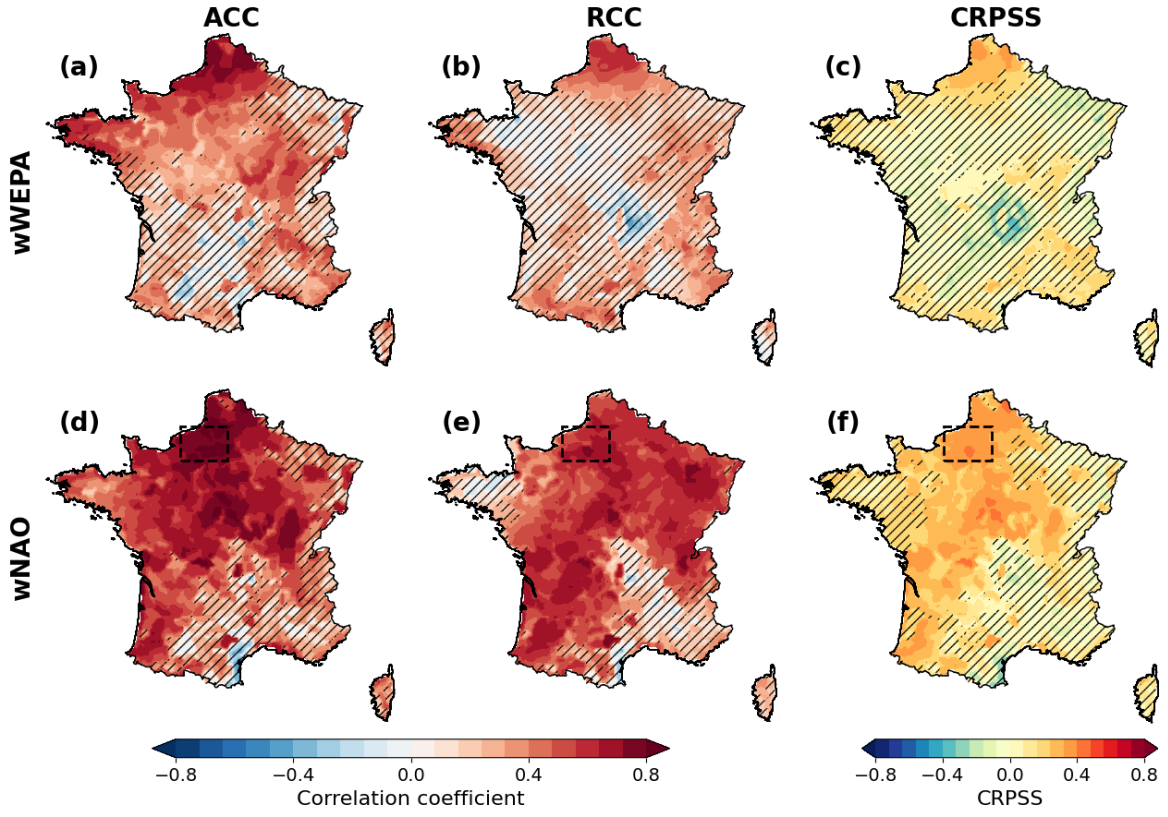

Fig. 8: Forecast skill for 8-year mean winter (ONDJFM) precipitation anomalies over France. Results are derived from subsampled hindcasts based on the wWEPA (a–c) and wNAO (d–f) indices. Panels show (a,d) Anomaly Correlation Coefficient (ACC), (b,e) Residual Correlation Coefficient (RCC)—quantifying skill beyond the forced response—and (c,f) Continuous Ranked Probability Skill Score (CRPSS), all computed against SAFRAN precipitation observations over 1966–2019. Hatched areas indicate region where skill scores are not statistically significant at the 95% confidence level, as assessed using a 1000 sample block bootstrap.

For winter, hindcasts subsampled on wWEPA yield significant ACC over 50% of all pixels, mainly over the northwestern France ($ACC \in [-0.39, 0.80]$ over all the pixels covering France; median $= 0.32$). RCC is significant over 24% of France, indicating that part of this skill is already present in the uninitialized ensemble ($RCC \in [-0.48, 0.64]$; median $= 0.19$). The probabilistic performance shows few localized gains, with significant CRPSS on 18% of the pixels ($CRPSS \in [-0.41, 0.37]$; median $= 0.03$). In contrast, hindcasts subsampled on wNAO exhibit substantial better skill, with significant ACC over 70% of the pixels, covering most of mainland France except the Mediterranean coast ($ACC \in [-0.51, 0.87]$; median $= 0.53$). RCC analysis ($RCC \in [-0.42, 0.77]$; median $= 0.53$) go in the same direction with 77% significant pixels and confirm that hindcasts subsampled on the wNAO provide significant skill improvements beyond the forced signal. Finally, CRPSS metric highlights the reduced ensemble spread of the prediction with 51% significant pixels ($CRPSS \in [-0.39, 0.46]$; median $= 0.19$). While both indices produce skillful predictions, those based on wNAO consistently outperform wWEPA. These results confirm wNAO as a more effective large-scale predictor for decadal winter precipitation.

https://doi.org/10.5194/egusphere-2026-573
Preprint. Discussion started: 27 February 2026

For summer, overall forecast skill is lower compared to winter (Fig. 9). Hindcasts subsampled according to sNAO yield meaningful but spatially fragmented skill, covering 10% of the French territory ($ACC \in [-0.55, 0.64]; \text{median} = 0.02$). Combining sNAO with uAMV index notably enhances performance by broadening skillful areas (ACC $\in [-0.48, 0.86]; \text{median} = 0.40,$ significant over 53% of France) and reducing ensemble uncertainty, consistent with RCC significant over 52% of France ($RCC \in [-0.61, 0.84]$) and confirmed by probabilistic improvements in CRPSS, with 43% significant pixels ($CRPSS \in [-0.53, 0.46], \text{median} = 0.13$). In contrast, hindcasts subsampled on sMedScand alone yields limited skill, with significant ACC covering only 3% of France and 19% after incorporating the uAMV. The lower skill of sMedScand-based subsampled hindcasts is consistent with weaker observed correlations and lower predictability for this index (Fig. 7, r=0.57). Overall, summer precipitation forecasts remain less skillful than winter counterparts, likely due to lower prediction skill of summer SLP indices and their reduced variability. For example, observed sNAO fluctuations remain within ±1 hPa, contrasting notably with broader amplitude ranges for winter wNAO (±4 hPa) and wWEPA (±2 hPa) (Fig. 7). Thus, we argue that the reduced summer skill likely arises from smaller SLP variability amplitudes (sNAO ±1 hPa vs wNAO ±4 hPa) and the predominance of localized convective rainfall not explicitly resolved in present-day models' frameworks.

https://doi.org/10.5194/egusphere-2026-573
Preprint. Discussion started: 27 February 2026

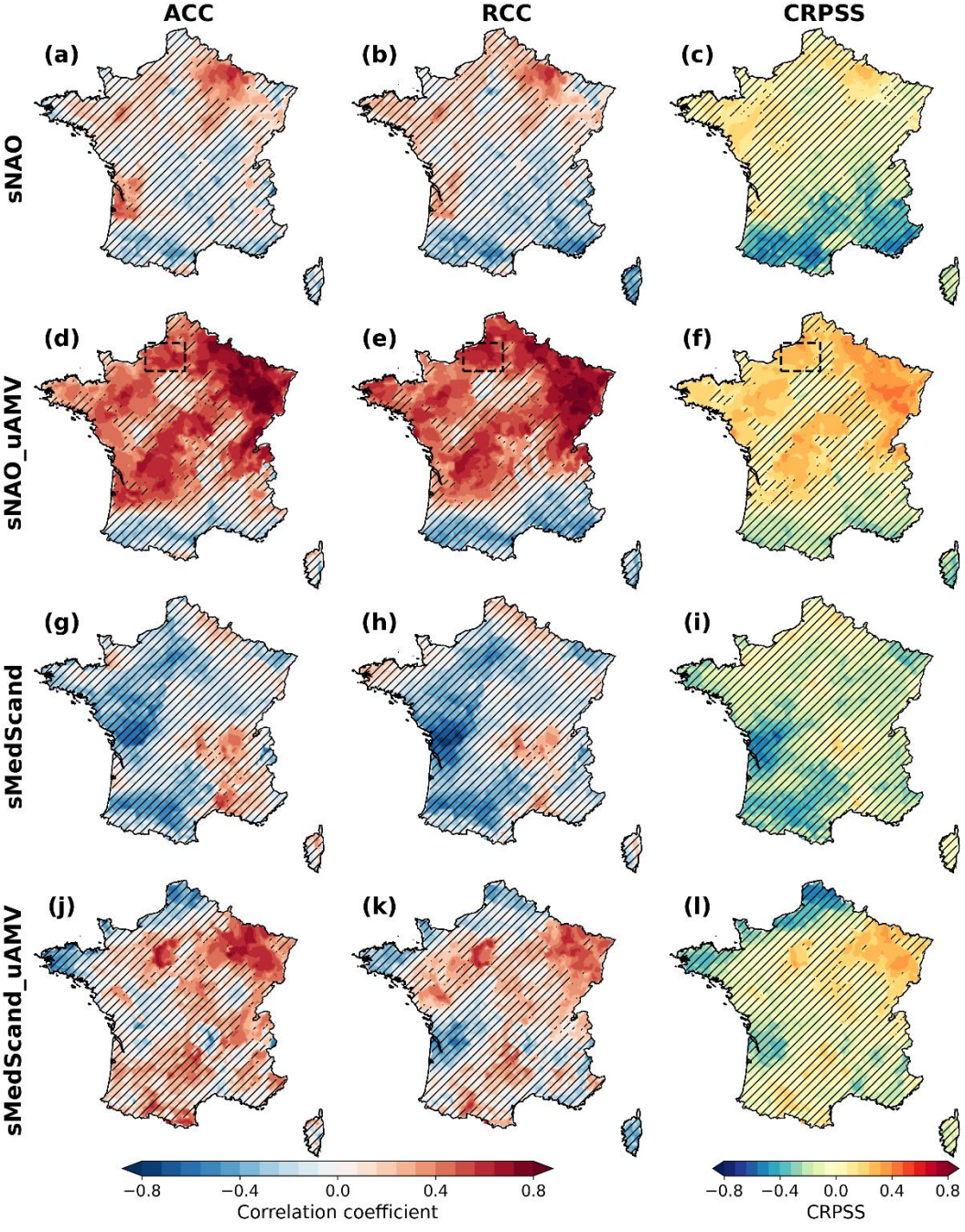

Fig. 9: Forecast skill for 8-year mean summer (AMJJAS) precipitation anomalies over France. Results are derived from subsampled hindcasts based on the sNAO (a–c), sNAO+uAMV (d-f), sMedScand (g-i) and sMedScand+uAMV (j-l) indices. Panels show (a,d) Anomaly Correlation Coefficient (ACC), (b,e) Residual Correlation Coefficient (RCC)—quantifying skill beyond the forced response—and (c,f) Continuous Ranked Probability Skill Score (CRPSS), all computed against SAFRAN precipitation observations over 1966–2019. Hatched regions indicate areas where skill scores are not statistically significant at the 95% confidence level, as assessed using a 1000 sample block bootstrap.

https://doi.org/10.5194/egusphere-2026-573
Preprint. Discussion started: 27 February 2026

In summary, wNAO-based subsampling for winter and combined sNAO+uAMV subsampling for summer yield most skillful decadal precipitation forecasts over France. For northern France (e.g. regions around Rouen, Figs. 8-9), correlation between predicted and observed 8-year precipitation anomalies improve compared to the uninitialized hindcasts from 0.68 to 0.83 in winter, and from 0.02 to 0.58 in summer (Fig. 10). Furthermore, the ensemble spread is notably reduced in the subsampled hindcasts, indicating lower prediction uncertainty and greater confidence compared to the broader uninitialized ensemble. These results demonstrate the tangible benefits of index-based subsampling for operational decadal climate forecasting.

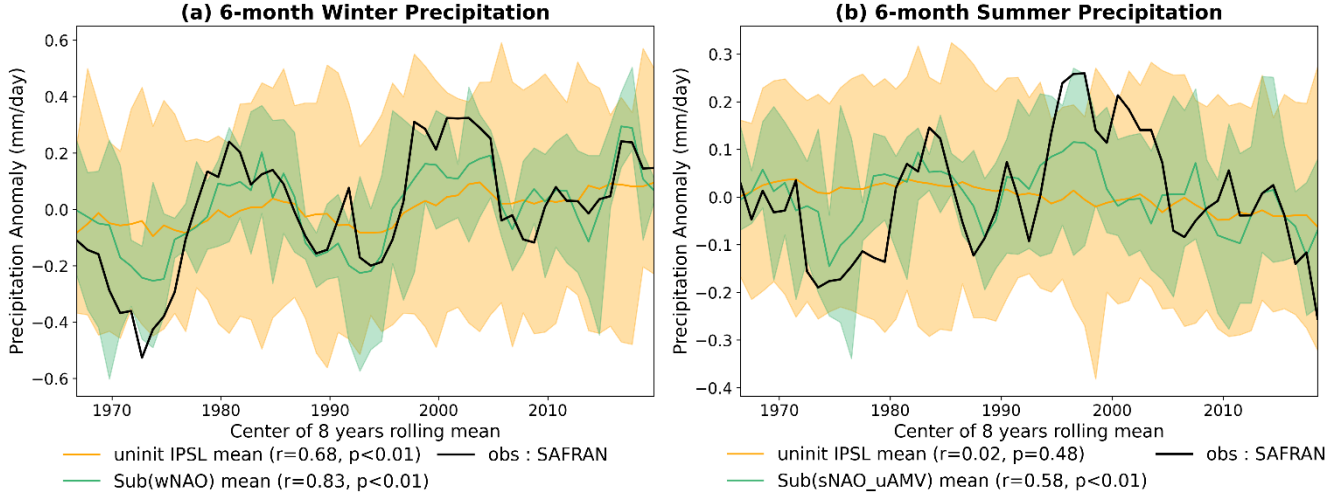

Fig. 10: Panel (a) and (b) show 8-year running mean precipitation anomalies for winter (ONDJFM) and summer (AMJJAS), respectively, averaged over the region outlined by dashed boxes in Figs. 8 and 9. The black line shows SAFRAN observations. The green line represents the mean of the five-member sub-ensemble selected based on the wNAO index (panel a) and combined sNAO+uAMV indices (panel b). The yellow line shows the mean of the full uninitialized IPSL ensemble. Shaded areas indicate the ensemble spread, defined as the 5th to 95th percentile range.

3.4 Sensitivity and robustness

The skill of the prediction system proposed here in Fig. 1 relies on the choice of several key parameters, including the averaging window length. Recent study show that winter NAO boosted decadal predictions can achieve skillful forecasts starting from 4- or 5-year averages (Alkama et al., sub.). Using 5-year means instead of 8-year averages yields slightly reduced but still meaningful skill for wNAO in winter and and sNAO+uAMV in summer (see Supplementary S7).

Combining the uAMV index with summer SLP indices improved precipitation predictions. This aligns with recent studies reporting benefits from including SST-based indices in winter forecasts (Bonnet et al., 2025; Nicolì et al., 2025). We also evaluated combinations of wNAO and wWEPA with uAMV (See Supplementary S4), as well as SST averages over the subpolar Gyre, but found no significant improvement.

Similarly, varying the sub-ensemble size between two and eight members reveals an optimal compromise around five members for the sNAo+uAMV-based subsampling, balancing ensemble mean correlation with predictive uncertainty (See

https://doi.org/10.5194/egusphere-2026-573
Preprint. Discussion started: 27 February 2026

Supplementary S8). This optimum is specific to this multi-criteria subsampling. In this study, a fixed sub-ensemble size of five members is used across all subsampling experiments to ensure consistency and comparability.

On the selection of potential SLP indices, we attempted to study both SLP and precipitation variability simultaneously using the Maximum Covariance Analysis (MCA) method. Results were similar in summer, but more ambiguous in winter, with a switch between the first two modes between the MCA and precipitation EOFs. The interpretation of the modes resulting from the MCA is however challenging since they maximize the coverability and are not orthogonal. This is why we preferred to use EOF approach.

Additional indices (see Supplementary S5), including the classic NAO index defined as the Iceland-Azores dipole and a Europe North-South (EUNS) index related to winter precipitation PC2, were also tested but yield no improvements for precipitation, compared to the results shown here, despite the higher decadal prediction skill of the NAO.

4 Discussion and conclusions

This study demonstrates the potential for skillful decadal precipitation predictions over France both in summer and winter, through a prediction system based on decadal predictions from DCPP as well as subsampling techniques. This system is leveraging large-scale atmospheric and oceanic teleconnections related to the French climate, but the methodology can be extended and applied to any other regions of the globe. More precisely, the principle is to perform a combination of EOF and wavelet analyses, to evaluate if both winter and summer precipitation (here over France) exhibit significant multi-annual to multi-decadal variability linked to dominant modes of North Atlantic variability. These analyses guide the identification of physically meaningful predictors—such as the North Atlantic Oscillation (wNAO) and West Europe Pressure Anomaly (wWEPA) for winter, and the Summer NAO (sNAO) and Mediterranean-Scandinavia (sMedScand) indices for summer—which form the foundation of our prediction system.

We then use the decadal forecasts of those predictors based on the DCPP database and with a boosted skill score based on Alkama et al. (sub.) methodology. Results from this approach are then combined with a subsampling method that selects members from a large uninitialized climate model ensemble consistent with the large-scale variability mode predicted by the Alkama et al. (sub.) approach.

The resulting predictions of precipitation over France do show some skills which are outperforming the uninitialized simulations. The forecast skill of the indices themselves, as well as their representation and relationship with regional precipitation in climate models, critically influence the quality of precipitation forecasts after subsampling. For example, although WEPA-like indices are closely associated with the principal mode of precipitation variability, wNAO-based subsampling consistently produces higher skills in precipitation predictions, likely due to the larger amplitude of the NAO predicted signal. These differences become particularly evident when comparing seasonal performance. Winter forecasts clearly outperform summer forecasts, reflecting the strong low-frequency predictability of winter circulation over the North

https://doi.org/10.5194/egusphere-2026-573
Preprint. Discussion started: 27 February 2026

Atlantic. Summer precipitation is actually shaped by more localized and convective processes, which are less well captured in coarse resolution model, while in winter, convective events are scarcer. Nevertheless, incorporating multiple predictors especially by combining sNAO and the Atlantic Multidecadal Variability (AMV) substantially enhanced summer forecast skill. An important methodological note is that our AMV (called here uAMV) retains the externally forced component rather than isolating internal variability, which is why we called it uAMV. Keeping the forced signal allows the prediction to be constrained by both internal variability and the forced trend, which means that the observed improvement in forecast skill may result from constraining either one or both. Disentangling these contributions requires further investigation left for future studies.

Our results confirm and extend previous findings demonstrating that improved predictions of large-scale climate indices, such as the boosted NAO forecasts developed by Alkama et al. (sub.), can be effectively leveraged to enhance regional hydroclimate predictions (Nicolì et al., 2025; Tsartsali et al., 2023). While earlier studies focused primarily on winter NAO and its influence, our work broadens this scope to include both winter and summer seasons, incorporating combined index approaches such as the sNAO, together with the uAMV index for summer precipitation forecasting. This highlights the added value of integrating multiple atmospheric and oceanic drivers to capture complex seasonal precipitation variability. Importantly, the novel workflow developed here integrates subsampling of ensemble members from the uninitialized IPSL-CM6A-LR model based on these boosted index forecasts, followed by bias correction using the CDF-t downscaling to the high-resolution (8 km) SAFRAN observational grid. Therefore, the prediction system presented here not only improves forecast skill but also provides operationally relevant, high-resolution decadal precipitation predictions over France, offering a significant advance towards actionable climate services.

While these findings offer promising advances for regional climate services and water management applications, several challenges remain. Precipitation prediction skill is primarily constrained by the limited forecasting performance of some SLP indices (See Supplementary S3). In addition, the uninitialized large ensemble used for subsampling is characterized by a relatively coarse spatial resolution of approximately 250 × 150 km. Although statistical downscaling to 8 km improves spatial detail, it likely does not fully capture fine-scale temporal variability at that resolution. Despite the generally satisfactory results obtained here, employing higher-resolution climate models could further enhance the representation of small-scale spatial structures. The predictive skill may also be sensitive to the choice of the uninitialized ensemble, suggesting that larger or more diverse ensembles could be explored. Moreover, an SLP index that does not yield skillful predictions with the IPSL-CM6A-LR may still serve as a valuable predictor for other models. While this evaluation covers the entire historical period, skill may vary over time. This highlights the possibility to identify potential windows of opportunity with better predictability, for instance due to large SLP indices or AMV variations (e.g. Sgubin et al., 2021). The focus on 8-year averages suits decadal-scale planning but may mask shorter-term dynamics relevant for some stakeholders. Preliminary results for 5-year averages suggest modest, yet significant skill, warranting further investigation. Future work should explore adaptive seasonal definitions, integration of additional indices, optimal weighting strategies and improved choice of the uninitialized model ensemble (e.g. other model ensemble, or larger one) to further enhance predictive skill.

https://doi.org/10.5194/egusphere-2026-573
Preprint. Discussion started: 27 February 2026

Operationalizing this framework poses practical challenges, including coordination across multiple modeling centers and managing ensemble sizes and parameter choices within the subsampling procedure. Although the current ensemble size of five members balances skill and uncertainty, further optimization and sensitivity analyses are desirable.

In conclusion, our study presents a coherent and robust methodology that improves decadal-scale precipitation prediction over France at high spatial resolution. By combining advanced atmospheric and oceanic index predictions with targeted subsampling and bias correction, we achieve enhanced skill and reduced uncertainty, valuable for climate adaptation strategies. The presented methodology, summed up in Fig.1 can potentially be developed for other countries or regions and may also substantially improve prediction skill there. Furthermore, extending this framework to other climate variables and precipitation indicators, such as extreme events and droughts, represents a natural next step, given their large impacts for various stakeholders. These developments will be instrumental for reliable climate services that support informed decision-making based on improved prediction of climate variability and change at the decadal time scale.

Appendix A

Table A1: List of DCPP-A climate models included in this study.

Model	Ensemble size
BCC-CSM2-MR	8
CESM1-1-CAM5-CMIP5	40
CMCC-CM2-SR5	20
CanESM5	20
EC-Earth3	15
FGOALS-f3-L	9
HadGEM3-GC31-MM	10
IPSL-CM6A-LR	10
MIROC6	10
MPI-ESM1-2-HR	10
MPI-ESM1-2-LR	16
NorCPM1	20

Appendix B

- **ACC:** Pearson correlation coefficient is computed on predicted ensemble mean and observed anomalies:

$$ACC = \frac{\sum_{i=1}^{N}(f_i-\bar{f})(o_i-\bar{o})}{\sum_{i=1}^{N}(f_i-\bar{f})^2 \sum_{i=1}^{N}(o_i-\bar{o})^2} \quad (1)$$

https://doi.org/10.5194/egusphere-2026-573
Preprint. Discussion started: 27 February 2026

Where N indicates the time series length, f_i and $\bar{f}$ (respectively o_i and $\bar{o}$) are ensemble mean forecast anomalies (respectively observation anomalies) at time step i and average over the whole time series, respectively.

- **RCC:** Correlation coefficients are computed on residuals o' and f' representing the variability that cannot be captured by the uninitialized simulations. Residuals are estimated as follow:

$$o' = o - r_{ou}\frac{\sigma_o}{\sigma_u}u \quad \text{and} \quad f' = f - r_{fu}\frac{\sigma_f}{\sigma_u}u \tag{2}$$

Where u is the uninitialized ensemble mean, σ_u, σ_f and σ_o are the standard deviations of u, f and o and r_{ou} and r_{fu} are the correlations between o and u and between f and u respectively (Smith et al., 2019).

- **CRPS:** The instantaneous CRPS is computed as each time step, then averaged over the all period. It is defined as the quadratic measure of discrepancy between the forecast Cumulative Distribution Function (CDF) (F) and the empirical CDF of the observation (o):

$$crps(F,o) = \int_{\mathbb{R}} [F(x) - \mathbb{1}(x \geq o)]^2 \, dx \tag{3}$$

Here estimated as:

$$CRPS(x,o)_t = \frac{\sum_{i=1}^{M}(|x_i - o|)}{M} - \frac{\sum_{i=1}^{M}\sum_{j=1}^{M}(|x_i - x_j|)}{2K} \tag{4}$$

With M the ensemble size, x the predicted values ensemble and o the observed value at time step t. Here we use the *fair* estimation, so $K = M(M-1)$. CRPS ranges from 0 to $+\infty$, where values close to 1 indicate skill.

- **CRPSS:** This score compares CRPS results between the selected sub-ensemble, and the full uninitialized large ensemble from IPSL-CM6A-LR.

$$CRPSS = 1 - \frac{\overline{CRPS_{sub}}}{\overline{CRPS_{uninit}}} \tag{5}$$

CRPSS ranges from $-\infty$ to 1, with positive values indicating that the sub-ensemble outperforms the reference ensemble.

Data availability

All CMIP6 (historical and DCPP simulations) data are available through the Earth System Grid Federation (ESGF; https://aims2.llnl.gov/search). ERA5 reanalysis data are available from the Copernicus Climate Data Store (https://cds.climate.copernicus.eu/datasets/reanalysis-era5-single-levels?tab=download). SAFRAN dataset is available from the French public data repository data.gouv at https://www.data.gouv.fr/datasets/donnees-changement-climatique-sim-quotidienne.

https://doi.org/10.5194/egusphere-2026-573
Preprint. Discussion started: 27 February 2026

Code availability

The code used to produce the results reported in this paper is available from the corresponding author upon reasonable request.

Author contributions

All authors designed the study and developed the method. RA and JC developed the source code. JC generated all figures and conducted the analysis. All the authors contributed to interpreting the results, discussing the findings. JC wrote the manuscript with contributions from all co-authors.

Competing interests

The authors declare that they have no conflict of interest.

Acknowledgements

To process the CMIP6 data, this study benefited from the IPSL mesocenter ESPRI facility which is supported by CNRS, UPMC, Labex L-IPSL, CNES and Ecole Polytechnique. We acknowledge the use of the AI language model ChatGPT to assist with English language editing and formulation improvements. Finally, we thank all colleagues and collaborators who contributed valuable discussions and insights that improved this study.

Financial Support

This project was funded by the French State as part of France 2030 operated by ADEME. This study received financial support from the French government in the framework of the University of Bordeaux's IdEx "Investments for the Future" program / RRI Tackling Global Change.

References

Alkama, R., Swingedouw, D., Mignot, J., Gastineau, G., and Ogée, J.: Clearing the noise to predict the rhythm of the North Atlantic climate, Submitted to Science Advances., sub.

Boer, G. J., Smith, D. M., Cassou, C., Doblas-Reyes, F., Danabasoglu, G., Kirtman, B., Kushnir, Y., Kimoto, M., Meehl, G. A., Msadek, R., Mueller, W. A., Taylor, K. E., Zwiers, F., Rixen, M., Ruprich-Robert, Y., and Eade, R.: The Decadal Climate Prediction Project (DCPP) contribution to CMIP6, Geoscientific Model Development, 9, 3751–3777, https://doi.org/10.5194/gmd-9-3751-2016, 2016.

https://doi.org/10.5194/egusphere-2026-573
Preprint. Discussion started: 27 February 2026

Bonnet, R., Boucher, O., Deshayes, J., Gastineau, G., Hourdin, F., Mignot, J., Servonnat, J., and Swingedouw, D.: Presentation and Evaluation of the IPSL-CM6A-LR Ensemble of Extended Historical Simulations, Journal of Advances in Modeling Earth Systems, 13, e2021MS002565, https://doi.org/10.1029/2021MS002565, 2021.

Bonnet, R., Boé, J., Sanchez-Gomez, E., and Cassou, C.: Reduction of uncertainty in near-term climate forecast by combining observations and decadal predictions, https://doi.org/10.5194/egusphere-2025-4463, 24 September 2025.

Borchert, L. F., Menary, M. B., Swingedouw, D., Sgubin, G., Hermanson, L., and Mignot, J.: Improved Decadal Predictions of North Atlantic Subpolar Gyre SST in CMIP6, Geophysical Research Letters, 48, e2020GL091307, https://doi.org/10.1029/2020GL091307, 2021.

Börgel, F., Meier, H. E. M., Gröger, M., Rhein, M., Dutheil, C., and Kaiser, J. M.: Atlantic multidecadal variability and the implications for North European precipitation, Environ. Res. Lett., 17, 044040, https://doi.org/10.1088/1748-9326/ac5ca1, 2022.

Casanueva, A., Rodríguez-Puebla, C., Frías, M. D., and González-Reviriego, N.: Variability of extreme precipitation over Europe and its relationships with teleconnection patterns, Hydrology and Earth System Sciences, 18, 709–725, https://doi.org/10.5194/hess-18-709-2014, 2014.

Castelle, B., Dodet, G., Masselink, G., and Scott, T.: A new climate index controlling winter wave activity along the Atlantic coast of Europe: The West Europe Pressure Anomaly, Geophysical Research Letters, 44, 1384–1392, https://doi.org/10.1002/2016GL072379, 2017.

Dawson, A.: eofs: A Library for EOF Analysis of Meteorological, Oceanographic, and Climate Data | Journal of Open Research Software, https://doi.org/10.5334/jors.122, 2016.

Dong, B., Sutton, R. T., Woollings, T., and Hodges, K.: Variability of the North Atlantic summer storm track: mechanisms and impacts on European climate, Environ. Res. Lett., 8, 034037, https://doi.org/10.1088/1748-9326/8/3/034037, 2013.

Dunstone, N., Lockwood, J., Solaraju-Murali, B., Reinhardt, K., Tsartsali, E. E., Athanasiadis, P. J., Bellucci, A., Brookshaw, A., Caron, L.-P., Doblas-Reyes, F. J., Früh, B., González-Reviriego, N., Gualdi, S., Hermanson, L., Materia, S., Nicodemou, A., Nicolì, D., Pankatz, K., Paxian, A., Scaife, A., Smith, D., and Thornton, H. E.: Towards Useful Decadal Climate Services, https://doi.org/10.1175/BAMS-D-21-0190.1, 2022.

Dunstone, N., Smith, D. M., Hardiman, S. C., Hermanson, L., Ineson, S., Kay, G., Li, C., Lockwood, J. F., Scaife, A. A., Thornton, H., Ting, M., and Wang, L.: Skilful predictions of the Summer North Atlantic Oscillation, Commun Earth Environ, 4, 1–11, https://doi.org/10.1038/s43247-023-01063-2, 2023.

Durand, Y., Brun, E., Merindol, L., Guyomarc'h, G., Lesaffre, B., and Martin, E.: A meteorological estimation of relevant parameters for snow models, Annals of Glaciology, 18, 65–71, https://doi.org/10.3189/S0260305500011277, 1993.

Ferro, C. a. T.: Fair scores for ensemble forecasts, Quarterly Journal of the Royal Meteorological Society, 140, 1917–1923, https://doi.org/10.1002/qj.2270, 2014.

Folland, C. K., Knight, J., Linderholm, H. W., Fereday, D., Ineson, S., and Hurrell, J. W.: The Summer North Atlantic Oscillation: Past, Present, and Future, Journal of Climate, 22, 1082–1103, https://doi.org/10.1175/2008JCLI2459.1, 2009.

Friter, N., Massei, N., Laignel, B., Durand, A., Dieppois, B., and Deloffre, J.: Links between NAO fluctuations and inter-annual variability of winter-months precipitation in the Seine River watershed (north-western France), Comptes Rendus. Géoscience, 344, 396–405, https://doi.org/10.1016/j.crte.2012.07.004, 2012.

https://doi.org/10.5194/egusphere-2026-573
Preprint. Discussion started: 27 February 2026

Gneiting, T. and Raftery, A. E.: Strictly Proper Scoring Rules, Prediction, and Estimation, Journal of the American Statistical Association, 102, 359–378, https://doi.org/10.1198/016214506000001437, 2007.

Goddard, L., Kumar, A., Solomon, A., Smith, D., Boer, G., Gonzalez, P., Kharin, V., Merryfield, W., Deser, C., Mason, S. J., Kirtman, B. P., Msadek, R., Sutton, R., Hawkins, E., Fricker, T., Hegerl, G., Ferro, C. A. T., Stephenson, D. B., Meehl, G. A., Stockdale, T., Burgman, R., Greene, A. M., Kushnir, Y., Newman, M., Carton, J., Fukumori, I., and Delworth, T.: A verification framework for interannual-to-decadal predictions experiments, Clim Dyn, 40, 245–272, https://doi.org/10.1007/s00382-012-1481-2, 2013.

Gogien, F., Dechesne, M., Martinerie, R., and Lipeme Kouyi, G.: Assessing the impact of climate change on Combined Sewer Overflows based on small time step future rainfall timeseries and long-term continuous sewer network modelling, Water Research, 230, 119504, https://doi.org/10.1016/j.watres.2022.119504, 2023.

Hawkins, E. and Sutton, R.: The potential to narrow uncertainty in projections of regional precipitation change, Clim Dyn, 37, 407–418, https://doi.org/10.1007/s00382-010-0810-6, 2011.

Hermanson, L., Smith, D., Seabrook, M., Bilbao, R., Doblas-Reyes, F., Tourigny, E., Lapin, V., Kharin, V. V., Merryfield, W. J., Sospedra-Alfonso, R., Athanasiadis, P., Nicoli, D., Gualdi, S., Dunstone, N., Eade, R., Scaife, A., Collier, M., O'Kane, T., Kitsios, V., Sandery, P., Pankatz, K., Früh, B., Pohlmann, H., Müller, W., Kataoka, T., Tatebe, H., Ishii, M., Imada, Y., Kruschke, T., Koenigk, T., Karami, M. P., Yang, S., Tian, T., Zhang, L., Delworth, T., Yang, X., Zeng, F., Wang, Y., Counillon, F., Keenlyside, N., Bethke, I., Lean, J., Luterbacher, J., Kolli, R. K., and Kumar, A.: WMO Global Annual to Decadal Climate Update: A Prediction for 2021–25, Bulletin of the American Meteorological Society, 103, E1117–E1129, https://doi.org/10.1175/BAMS-D-20-0311.1, 2022.

Hersbach, H.: Decomposition of the Continuous Ranked Probability Score for Ensemble Prediction Systems, 2000.

Hersbach, H., Bell, B., Berrisford, P., Hirahara, S., Horányi, A., Muñoz-Sabater, J., Nicolas, J., Peubey, C., Radu, R., Schepers, D., Simmons, A., Soci, C., Abdalla, S., Abellan, X., Balsamo, G., Bechtold, P., Biavati, G., Bidlot, J., Bonavita, M., De Chiara, G., Dahlgren, P., Dee, D., Diamantakis, M., Dragani, R., Flemming, J., Forbes, R., Fuentes, M., Geer, A., Haimberger, L., Healy, S., Hogan, R. J., Hólm, E., Janisková, M., Keeley, S., Laloyaux, P., Lopez, P., Lupu, C., Radnoti, G., de Rosnay, P., Rozum, I., Vamborg, F., Villaume, S., and Thépaut, J.-N.: The ERA5 global reanalysis, Quarterly Journal of the Royal Meteorological Society, 146, 1999–2049, https://doi.org/10.1002/qj.3803, 2020.

Hurrell, J. W. and Deser, C.: North Atlantic climate variability: The role of the North Atlantic Oscillation, Journal of Marine Systems, 79, 231–244, https://doi.org/10.1016/j.jmarsys.2009.11.002, 2010.

Hutchins, B. W., Brayshaw, D. J., Shaffrey, L. C., Thornton, H. E., and Smith, D. M.: Decadal Prediction for the European Energy Sector, Meteorological Applications, 32, e70054, https://doi.org/10.1002/met.70054, 2025.

Jalón-Rojas, I. and Castelle, B.: Climate Control of Multidecadal Variability in River Discharge and Precipitation in Western Europe, Water, 13, 257, https://doi.org/10.3390/w13030257, 2021.

Jianping, L. and Wang, J. X. L.: A new North Atlantic Oscillation index and its variability, Adv. Atmos. Sci., 20, 661–676, https://doi.org/10.1007/BF02915394, 2003.

Kharin, V. V., Boer, G. J., Merryfield, W. J., Scinocca, J. F., and Lee, W.-S.: Statistical adjustment of decadal predictions in a changing climate, Geophysical Research Letters, 39, https://doi.org/10.1029/2012GL052647, 2012.

Kharin, V. V., Zwiers, F. W., Zhang, X., and Wehner, M.: Changes in temperature and precipitation extremes in the CMIP5 ensemble, Climatic Change, 119, 345–357, https://doi.org/10.1007/s10584-013-0705-8, 2013.

https://doi.org/10.5194/egusphere-2026-573
Preprint. Discussion started: 27 February 2026

Knight, J. R., Folland, C. K., and Scaife, A. A.: Climate impacts of the Atlantic Multidecadal Oscillation, Geophysical Research Letters, 33, https://doi.org/10.1029/2006GL026242, 2006.

Krieger, S. and Freij, N.: PyCWT: spectral analysis using wavelets in Python, 2023.

Labrousse, C., Ludwig, W., Pinel, S., Sadaoui, M., and Lacquement, G.: Unravelling Climate and Anthropogenic Forcings on the Evolution of Surface Water Resources in Southern France, Water, 12, 3581, https://doi.org/10.3390/w12123581, 2020.

Le Moigne, P., Besson, F., Martin, E., Boé, J., Boone, A., Decharme, B., Etchevers, P., Faroux, S., Habets, F., Lafaysse, M., Leroux, D., and Rousset-Regimbeau, F.: The latest improvements with SURFEX v8.0 of the Safran–Isba–Modcou hydrometeorological model for France, Geoscientific Model Development, 13, 3925–3946, https://doi.org/10.5194/gmd-13-3925-2020, 2020.

Leeuwenburg, T., Loveday, N., Ebert, E. E., Cook, H., Khanarmuei, M., Taggart, R. J., Ramanathan, N., Carroll, M., Chong, S., Griffiths, A., and Sharples, J.: scores: A Python package for verifying and evaluating models and predictions with xarray, Journal of Open Source Software, 9, 6889, https://doi.org/10.21105/joss.06889, 2024.

Lockwood, J. F., Dunstone, N., Hermanson, L., Saville, G. R., Scaife, A. A., Smith, D., and Thornton, H. E.: A Decadal Climate Service for Insurance: Skillful Multiyear Predictions of North Atlantic Hurricane Activity and U.S. Hurricane Damage, https://doi.org/10.1175/JAMC-D-22-0147.1, 2023.

Marcheggiani, A., Robson, J., Monerie, P.-A., Bracegirdle, T. J., and Smith, D.: Decadal Predictability of the North Atlantic Eddy-Driven Jet in Winter, Geophysical Research Letters, 50, e2022GL102071, https://doi.org/10.1029/2022GL102071, 2023.

Meehl, G. A., Goddard, L., Murphy, J., Stouffer, R. J., Boer, G., Danabasoglu, G., Dixon, K., Giorgetta, M. A., Greene, A. M., Hawkins, E., Hegerl, G., Karoly, D., Keenlyside, N., Kimoto, M., Kirtman, B., Navarra, A., Pulwarty, R., Smith, D., Stammer, D., and Stockdale, T.: Decadal Prediction: Can It Be Skillful?, Bull. Amer. Meteor. Soc., 90, 1467–1486, https://doi.org/10.1175/2009BAMS2778.1, 2009.

Michel, S. L. L., Swingedouw, D., Ortega, P., Gastineau, G., Mignot, J., McCarthy, G., and Khodri, M.: Early warning signal for a tipping point suggested by a millennial Atlantic Multidecadal Variability reconstruction, Nat Commun, 13, 5176, https://doi.org/10.1038/s41467-022-32704-3, 2022.

Michelangeli, P.-A., Vrac, M., and Loukos, H.: Probabilistic downscaling approaches: Application to wind cumulative distribution functions, Geophysical Research Letters, 36, https://doi.org/10.1029/2009GL038401, 2009.

Moulds, S., Slater, L. J., Dunstone, N. J., and Smith, D. M.: Skillful Decadal Flood Prediction, Geophysical Research Letters, 50, e2022GL100650, https://doi.org/10.1029/2022GL100650, 2023.

Msadek, R., Dixon, K. W., Delworth, T. L., and Hurlin, W.: Assessing the predictability of the Atlantic meridional overturning circulation and associated fingerprints, Geophysical Research Letters, 37, https://doi.org/10.1029/2010GL044517, 2010.

Nicolì, D., Gualdi, S., and Athanasiadis, P. J.: Decadal predictions outperform climate projections in forecasting Mediterranean wintertime precipitation, Environ. Res. Lett., 20, 034034, https://doi.org/10.1088/1748-9326/adb59e, 2025.

Paxian, A., Reinhardt, K., Pankatz, K., Pasternack, A., Lorza-Villegas, M. P., Scheibel, M., Hoff, A., Mannig, B., Lorenz, P., and Früh, B.: High-Resolution Decadal Drought Predictions for German Water Boards: A Case Study for the Wupper Catchment, Front. Clim., 4, https://doi.org/10.3389/fclim.2022.867814, 2022.

https://doi.org/10.5194/egusphere-2026-573
Preprint. Discussion started: 27 February 2026

Persechino, A., Mignot, J., Swingedouw, D., Labetoulle, S., and Guilyardi, E.: Decadal predictability of the Atlantic meridional overturning circulation and climate in the IPSL-CM5A-LR model, Clim Dyn, 40, 2359–2380, https://doi.org/10.1007/s00382-012-1466-1, 2013.

Polkova, I., Swingedouw, D., Hermanson, L., Köhl, A., Stammer, D., Smith, D., Kröger, J., Bethke, I., Yang, X., Zhang, L., Nicolì, D., Athanasiadis, P. J., Karami, M. P., Pankatz, K., Pohlmann, H., Wu, B., Bilbao, R., Ortega, P., Yang, S., Sospedra-Alfonso, R., Merryfield, W., Kataoka, T., Tatebe, H., Imada, Y., Ishii, M., and Matear, R. J.: Initialization shock in the ocean circulation reduces skill in decadal predictions of the North Atlantic subpolar gyre, Front. Clim., 5, https://doi.org/10.3389/fclim.2023.1273770, 2023.

Rousselet, G. A., Pernet, C. R., and Wilcox, R. R.: The Percentile Bootstrap: A Primer With Step-by-Step Instructions in R, Advances in Methods and Practices in Psychological Science, 4, 1–10, https://doi.org/10.1177/2515245920911881, 2021.

Sauquet, E., Evin, G., Siauve, S., Aissat, R., Arnaud, P., Bérel, M., Bonneau, J., Branger, F., Caballero, Y., Colléoni, F., Ducharne, A., Gailhard, J., Habets, F., Hendrickx, F., Héraut, L., Hingray, B., Huang, P., Jaouen, T., Jeantet, A., Lanini, S., Le Lay, M., Magand, C., Mimeau, L., Monteil, C., Munier, S., Perrin, C., Robelin, O., Rousset, F., Soubeyroux, J.-M., Strohmenger, L., Thirel, G., Tocquer, F., Tramblay, Y., Vergnes, J.-P., and Vidal, J.-P.: A large transient multi-scenario multi-model ensemble of future streamflow and groundwater projections in France, https://doi.org/10.5194/egusphere-2025-1788, 20 May 2025.

Schlesinger, M. E. and Ramankutty, N.: An oscillation in the global climate system of period 65–70 years, Nature, 367, 723–726, https://doi.org/10.1038/367723a0, 1994.

Seyedhashemi, H., Moatar, F., Vidal, J.-P., and Thiéry, D.: Past and future discharge and stream temperature at high spatial resolution in a large European basin (Loire basin, France), Earth System Science Data, 15, 2827–2839, https://doi.org/10.5194/essd-15-2827-2023, 2023.

Sgubin, G., Swingedouw, D., Borchert, L. F., Menary, M. B., Noël, T., Loukos, H., and Mignot, J.: Systematic investigation of skill opportunities in decadal prediction of air temperature over Europe, Clim Dyn, 57, 3245–3263, https://doi.org/10.1007/s00382-021-05863-0, 2021.

Simpson, I. R., Yeager, S. G., McKinnon, K. A., and Deser, C.: Decadal predictability of late winter precipitation in western Europe through an ocean–jet stream connection, Nat. Geosci., 12, 613–619, https://doi.org/10.1038/s41561-019-0391-x, 2019.

Smith, D. M., Eade, R., Scaife, A. A., Caron, L.-P., Danabasoglu, G., DelSole, T. M., Delworth, T., Doblas-Reyes, F. J., Dunstone, N. J., Hermanson, L., Kharin, V., Kimoto, M., Merryfield, W. J., Mochizuki, T., Müller, W. A., Pohlmann, H., Yeager, S., and Yang, X.: Robust skill of decadal climate predictions, npj Clim Atmos Sci, 2, 1–10, https://doi.org/10.1038/s41612-019-0071-y, 2019.

Smith, D. M., Scaife, A. A., Eade, R., Athanasiadis, P., Bellucci, A., Bethke, I., Bilbao, R., Borchert, L. F., Caron, L.-P., Counillon, F., Danabasoglu, G., Delworth, T., Doblas-Reyes, F. J., Dunstone, N. J., Estella-Perez, V., Flavoni, S., Hermanson, L., Keenlyside, N., Kharin, V., Kimoto, M., Merryfield, W. J., Mignot, J., Mochizuki, T., Modali, K., Monerie, P.-A., Müller, W. A., Nicolí, D., Ortega, P., Pankatz, K., Pohlmann, H., Robson, J., Ruggieri, P., Sospedra-Alfonso, R., Swingedouw, D., Wang, Y., Wild, S., Yeager, S., Yang, X., and Zhang, L.: North Atlantic climate far more predictable than models imply, Nature, 583, 796–800, https://doi.org/10.1038/s41586-020-2525-0, 2020.

Solaraju-Murali, B., Gonzalez-Reviriego, N., Caron, L.-P., Ceglar, A., Toreti, A., Zampieri, M., Bretonnière, P.-A., Samsó Cabré, M., and Doblas-Reyes, F. J.: Multi-annual prediction of drought and heat stress to support decision making in the wheat sector, npj Clim Atmos Sci, 4, 1–9, https://doi.org/10.1038/s41612-021-00189-4, 2021.

https://doi.org/10.5194/egusphere-2026-573
Preprint. Discussion started: 27 February 2026

Solaraju-Murali, B., Bojovic, D., Gonzalez-Reviriego, N., Nicodemou, A., Terrado, M., Caron, L.-P., and Doblas-Reyes, F. J.: How decadal predictions entered the climate services arena: an example from the agriculture sector, Climate Services, 27, 100303, https://doi.org/10.1016/j.cliser.2022.100303, 2022.

Sutton, R. T. and Hodson, D. L. R.: Atlantic Ocean Forcing of North American and European Summer Climate, Science, 309, 115–118, https://doi.org/10.1126/science.1109496, 2005.

Swingedouw, D., Rodehacke, C. B., Behrens, E., Menary, M., Olsen, S. M., Gao, Y., Mikolajewicz, U., Mignot, J., and Biastoch, A.: Decadal fingerprints of freshwater discharge around Greenland in a multi-model ensemble, Clim Dyn, 41, 695–720, https://doi.org/10.1007/s00382-012-1479-9, 2013.

Swingedouw, D., Ortega, P., Mignot, J., Guilyardi, E., Masson-Delmotte, V., Butler, P. G., Khodri, M., and Séférian, R.: Bidecadal North Atlantic ocean circulation variability controlled by timing of volcanic eruptions, Nat Commun, 6, 6545, https://doi.org/10.1038/ncomms7545, 2015.

Terray, L.: Evidence for multiple drivers of North Atlantic multi-decadal climate variability, Geophysical Research Letters, 39, https://doi.org/10.1029/2012GL053046, 2012.

Torrence, C. and Compo, G. P.: A Practical Guide to Wavelet Analysis, Bull. Amer. Meteor. Soc., 79, 61–78, https://doi.org/10.1175/1520-0477(1998)079<0061:APGTWA>2.0.CO;2, 1998.

Trenberth, K. E. and Shea, D. J.: Atlantic hurricanes and natural variability in 2005, Geophysical Research Letters, 33, https://doi.org/10.1029/2006GL026894, 2006.

Tsartsali, E. E., Athanasiadis, P. J., Materia, S., Bellucci, A., Nicolì, D., and Gualdi, S.: Predicting precipitation on the decadal timescale: A prototype climate service for the hydropower sector, Climate Services, 32, 100422, https://doi.org/10.1016/j.cliser.2023.100422, 2023.

Vidal, J.-P., Martin, E., Franchistéguy, L., Habets, F., Soubeyroux, J.-M., Blanchard, M., and Baillon, M.: Multilevel and multiscale drought reanalysis over France with the Safran-Isba-Modcou hydrometeorological suite, Hydrology and Earth System Sciences, 14, 459–478, https://doi.org/10.5194/hess-14-459-2010, 2010.

Vrac, M., Drobinski, P., Merlo, A., Herrmann, M., Lavaysse, C., Li, L., and Somot, S.: Dynamical and statistical downscaling of the French Mediterranean climate: uncertainty assessment, Natural Hazards and Earth System Sciences, 12, 2769–2784, https://doi.org/10.5194/nhess-12-2769-2012, 2012.

Wang, L. and Ting, M.: Stratosphere-Troposphere Coupling Leading to Extended Seasonal Predictability of Summer North Atlantic Oscillation and Boreal Climate, Geophysical Research Letters, 49, e2021GL096362, https://doi.org/10.1029/2021GL096362, 2022.

Wilks, D. S.: Statistical methods in the atmospheric sciences, 4th edition., Elsevier, 2011.

World Meteorological Organization.: WMO Global Annual to Decadal Climate Update 2025-2029, WMO, 2024.